technische universität
dortmund

Edge-modes at interfaces between periodic media via reduced spatial dynamics near Dirac points

Ben Schweizer

Preprint 2026-01 April 2026

Fakultät für Mathematik
Technische Universität Dortmund
Vogelpothsweg 87
44227 Dortmund

Edge-modes at interfaces between periodic media via reduced spatial dynamics near Dirac points

Ben Schweizer[1]

27. April 2026

Abstract: We consider the Helmholtz operator in a d-dimensional waveguide, unbounded in x_1-direction. The unperturbed waveguide has periodic coefficients in x_1, the perturbations are different for $x_1 < 0$ and $x_1 > 0$. The perturbations are such that a band gap opens from a Dirac point. We show that an interface mode appears, corresponding to an eigenvalue in the band gap. Our proof uses the concept of reduced spatial dynamics and homogenization techniques. It is based on the analysis of the inhomogeneous problem for a right hand side that is a modulated eigenfunction of the unperturbed problem. We construct sequences of approximate solutions by solving ordinary differential equation; as these sequences are unbounded, we can conclude the existence of an eigenvalue.

Keywords: perturbation of periodic operators; band gap; surface mode; topological insulator; bulk-edge correspondance; Dirac point

MSC: 47A25, 78A40

1 Introduction

In a periodic medium, a self-adjoint differential operator has a spectrum that typically consists of bands and band gaps; this can be analyzed with the help of quasiperiodic solutions. When the periodicity is perturbed, the spectrum changes, bands and band gaps change their end-points, new gaps can be created. More fundamental changes of the spectrum can appear when the perturbed medium is no longer periodic. We think of the situation that a periodic medium is used on the two sides of an interface, but the media are not matching at the interface so that, globally, the medium is not periodic. In such a situation, an isolated eigenvalue can appear in a band gap. Our interest is to prove the existence of such isolated eigenvalues corresponding to interface modes.

We study the spectrum of elliptic operators in a waveguide $\Omega = \mathbb{R} \times \Sigma$, where $\Sigma \subset \mathbb{R}^{d-1}$ is a bounded domain that describes the cross-section of the waveguide in dimension $2 \leq d \in \mathbb{N}$. For coefficients $a, b : \Omega \to \mathbb{R}$, both 1-periodic in $x_1 \in \mathbb{R}$ and with a positive lower bound, we are interested in the spectral properties of the Helmholtz problem

$$-\nabla \cdot (a \nabla u) = \lambda \, b \, u \,. \tag{1.1}$$

[1]Technische Universität Dortmund, Fakultät für Mathematik, Vogelspothsweg 87, D-44227 Dortmund, ben.schweizer@tu-dortmund.de

Solutions are functions $u : \Omega \to \mathbb{C}$, the parameter $\lambda \in \mathbb{R}$ is the spectral parameter. We are interested in solutions for perturbations of a or b.

The starting point is an unperturbed problem in which (1.1) is considered with coefficients $a = a_0$ and $b = b_0$ that are both 1/2-periodic in direction $x_1 \in \mathbb{R}$. Obviously, we can regard this medium also as 1-periodic; when we do so, there typically appears a Dirac point at $k_0 = \pi$. We consider perturbations of the coefficients to new 1-periodic media that are no longer 1/2-periodic. This typically leads to the creation of a band gap from the Dirac point. In the construction of a single medium, say Medium I, we are interested in perturbations of the type $b^I_\varepsilon = b_0 + \varepsilon B^I$ and analogously for Medium II. To simplify notations, we will assume here always $a_0 \equiv 1$ and do not perturb this coefficient.

Our interest is to study a combined medium, using Medium I for $x_1 > 0$ and Medium II for $x_1 < 0$, for some $\varepsilon > 0$. We show the existence of a spectral parameter λ_ε in the spectral gap of the two 1-periodic media and the existence of an $L^2(\Omega)$-solution u_ε of (1.1) for the combined medium.

We next present the mathematical results of this paper. Subsection 1.1 contains a detailed description of a model system that meets all requirements of our mathematical result.

Assumption 1.1 (Structural assumptions on the media)**.** *Let the unperturbed coefficients* (a_0, b_0) *be* 1/2*-periodic with positive lower bounds. When considered as a* 1*-periodic medium, let* $k_0 = \pi$ *with* $\lambda_0 > 0$ *be a Dirac point and let* (1.1) *have exactly two linearly independent* k_0*-quasiperiodic homogeneous solutions for* $(a, b) = (a_0, b_0)$ *and* $\lambda = \lambda_0$*, we denote them as* V *and* W*. We assume that* V *has a non-vanishing flux* F *(defined in* (2.11)*).*

For every small parameter $\varepsilon > 0$*, let two* 1*-periodic media be given by* $(a^I_\varepsilon, b^I_\varepsilon)$ *and* $(a^{II}_\varepsilon, b^{II}_\varepsilon)$*. We assume that both are as described in Definition 2.1, in particular the differentiability of the b-coefficients with derivatives* B^I *and* B^{II}*. We assume for both media the symmetries (i) and (ii) of Assumption 2.2 and the relation* $B := B^I = -B^{II}$*. On the perturbation we demand* $\int_Y BV^2 \neq 0$*.*

Combined medium: As the coefficients of the combined medium we choose $(a_\varepsilon, b_\varepsilon)(x) = (a^I_\varepsilon, b^I_\varepsilon)(x)$ *for* $x_1 > 0$ *and* $(a_\varepsilon, b_\varepsilon)(x) = (a^{II}_\varepsilon, b^{II}_\varepsilon)(x)$ *for* $x_1 < 0$*.*

Our main result is that the existence of a spectral gap implies the existence of an interface eigenmode.

Theorem 1.2 (Existence of an interface mode)**.** *Let* $(a_\varepsilon, b_\varepsilon)$ *describe a combined medium as in Assumption 1.1. We assume that, for some* $\eta_0 > 0$*, both media* $(a^I_\varepsilon, b^I_\varepsilon)$ *and* $(a^{II}_\varepsilon, b^{II}_\varepsilon)$ *have, for every* $\varepsilon > 0$*, a spectral gap that contains the interval* $\Lambda_\varepsilon := (\lambda_0 - \varepsilon\eta_0, \lambda_0 + \varepsilon\eta_0)$*.*

Then, there exists a number $\varepsilon_0 > 0$ *such that, for every* $\varepsilon \in (0, \varepsilon_0)$*, the combined medium has an eigenvalue in the interval* Λ_ε *with eigenfunction* $u_\varepsilon \in L^2(\mathbb{R} \times \Sigma)$*.*

The assumption that the interval Λ_ε is contained in the spectral gap of Medium I means that, for every $\lambda \in \Lambda_\varepsilon$ and for the coefficients $(a^I_\varepsilon, b^I_\varepsilon)$, there is no quasiperiodic solution to the homogeneous problem (1.1). The statement of the theorem is that u_ε solves (1.1) for $(a_\varepsilon, b_\varepsilon)$ and some $\lambda_\varepsilon \in \Lambda_\varepsilon$.

1.1 A possible construction of a combined medium

In this subsection we construct a family of perturbed media to which the main theorem can be applied. We find the construction useful as an illustration and use it also in the numerical experiments.

We define media with "inclusions", illustrated by the dark discs in Figures 1, 3 and 5. Once inclusions are defined, we choose $b_0 \equiv 1$ outside the inclusions and b_0 larger than 1 in the inclusions; we recall that we choose $a_0 \equiv 1$. For 1/2-periodic inclusions, we obtain a 1/2-periodic medium. When we consider the 1/2-periodic medium as 1-periodic, the dispersion curves have a Dirac point in $k_0 = \pi$, we provide the argument in Section 2.2, see Figure 6 for dispersion curves.

For a parameter $\varepsilon > 0$, the perturbed coefficient b_ε is defined by shifts of the inclusions: The inclusion in the domain $(0, 1/2) \times \Sigma$ is shifted by ε to the left, the inclusion in the domain $(1/2, 1) \times \Sigma$ is shifted by ε to the right, see Figure 3. This defines the 1-periodic Medium I. Since it is not 1/2-periodic, the spectrum can have additional spectral gaps that are created out of the Dirac point. This is indeed the case, see the right part of Figure 7.

Medium II is constructed similarly, we now shift the inclusions towards each other instead of moving them away from each other. The combined medium is obtained by using Medium I for $x_1 > 0$ and Medium II for $x_1 < 0$, see Figure 1.

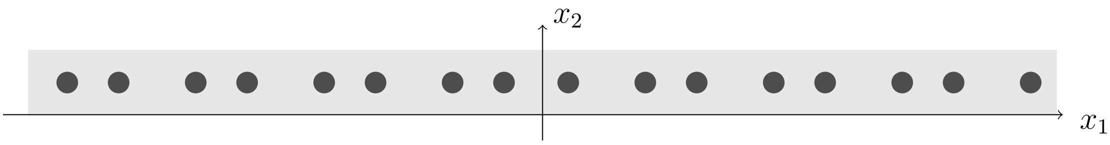

Figure 1: Sketch of the combined medium. On both sides of $x_1 = 0$, a 1-periodic medium is used. The 1-periodic media are identical up to a shift. The combined medium is not 1-periodic, since there is a mismatch at the interface $x_1 = 0$.

With this construction of b_ε, all assumptions of our main theorem can be satisfied. The assumptions on the Dirac point, on F and on the differentiability are discussed below. The symmetry (i) is satisfied by moving the inclusion in the right half-cell exactly as in the left half-cell, but in opposite direction. Also the reflection symmetry (ii) is satisfied by this construction when b_0 has the reflection symmetry. The relation $B^I = -B^{II}$ is also satisfied since we shift in opposite directions when we construct media I and II. Regarding $\int_Y BV^2 \neq 0$, we refer to the discussion in the last paragraph of Section 3.

Interface modes for the combined medium. We determine eigenvalues of the problem in the combined medium numerically by truncating the domain and imposing homogeneous Neumann boundary conditions at the left and the right boundaries of the domain. The numerics yield an eigenvalue that lies in the spectral gap of Medium I (or Medium II, which has the same spectrum). The corresponding eigenfunction is shown in Figure 2, it is localized at the interface.

There is a vast body of literature in physics about this effect. For λ in the spectral gap, Medium I and Medium II are both topological insulators, they have a different index. By the so-called "bulk-edge correspondance", there necessarily appears an

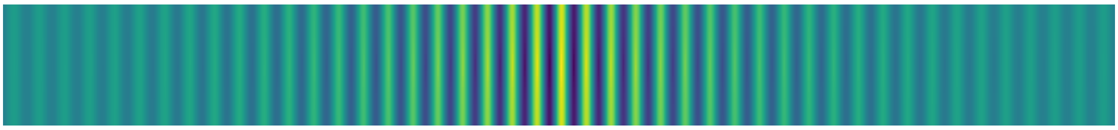

Figure 2: An eigenfunction in the strip for a combined medium with Neumann boundary conditions along all boundaries. The coordinates are x_1 and x_2, the aspect ratio is changed in order to show x_1 from -45 to $+45$. We see the interface mode, the eigenvalue $\lambda = 8.03$ is in the spectral gap of the media on the left and on the right, their geometry is generated with $r_0 = 0.25 \pm 0.03$.

interface mode (or edge-mode). We present an analytical proof for the existence of the interface mode, it is perturbative and not topological. Our proof uses standard analytical methods. We believe that the new concept of reduced spatial dynamics is of general interest and allows to find other new result in the field.

Remarks on the main result. We include some remarks regarding our assumptions and possible generalizations of the main result.

Remark 1: Symmetry assumptions (i) and (ii). The two symmetry requirements of Assumption 2.2 both regard the single periodic medium. Assumption (i) is the shift anti-symmetry $B(1/2 + x_1, \tilde{x}) = -B(x_1, \tilde{x})$. It is only used in order to simplify the expression for p in (5.8).

The reflection symmetry (ii) on b_ε is used at two points. It provides that the parameter q in (5.9) is real. Furthermore, it is used to derive the boundary conditions in the reduced dynamics.

We do not believe that the symmetries are fundamental for the observed effects. Indeed, in the numerical experiments, we construct b_ε-media with ellipsoidal inclusions in order to violate (ii), see Figure 4. The interface mode is, nonetheless, clearly present.

Remark 2: Symmetry in the media construction. Regarding the construction of the two media, we impose $B^I = -B^{II}$. This assumption is only made to simplify the proofs, it provides that the reduced dynamics uses the same parameters on the left and on the right.

Remark 3: Very different media in the two domains. In principle, our approach can also be used to analyze completely different media on the two sides of $x_1 = 0$. Our method still provides an ordinary differential equation on the two sides of the interface. One has to deal with the difficulty that different basis functions must be used on the two sides, we expect $u \approx \alpha_+ V_+ + \beta_+ W_+$ for $x_1 > 0$ and $u \approx \alpha_- V_- + \beta_- W_-$ for $x_1 < 0$, with $V_+ \neq V_-$ and/or $W_+ \neq W_-$. The challenge is to find conditions that relate $(\alpha_-, \beta_-)(0-)$ with $(\alpha_+, \beta_+)(0+)$.

Remark 4: Transition zone between the two media. As nicely illustrated in [5], one expects that a transition zone between the two media does not change the fact that there must exist an interface mode. Our method can still be used in such a setting, there appear problems that are similar to those sketched in Remark 3.

Remark 5: Non-waveguide geometries. Higher dimensional settings can be analyzed with our approach. One example is a medium in $\mathbb{R}^2$ that is derived from a medium that is 1-periodic in both directions x_1 and x_2. The perturbation is made such that different 1-periodic media are generated for $x_1 > 0$ and $x_1 < 0$. Our approach yields a reduced spatial dynamics for solutions $\alpha = \alpha(x_1, x_2)$ and $\beta = \beta(x_1, x_2)$. When we assume that these envelope functions are x_2-independent, the analysis of the reduced spatial dynamics is identical to the one presented here. We then obtain spectral values in the gap that are related to surface modes.

1.2 Literature

The wider field of our contribution is the spectral analysis of operators in media that are partially periodic. By partially periodic we mean that the medium (i.e., the coefficients in the partial differential equation) are chosen as one of the following: (a0) the medium is identical to a periodic medium outside a compact set, one often speaks of a compactly perturbed periodic medium. (a1) A periodic medium that is perturbed along a line (one-dimensional perturbation). (a2) A periodic medium that is perturbed along a hyperplane. (b) One uses one periodic medium on one side of a hyperplane, another periodic medium on the other side. The present article deals with (b). All the above geometries can be considered in the whole space or in subsets, of particular interest are waveguide geometries.

Existence theory. Simpler than a full spectral analysis is the existence theory for non-critical frequencies. We mention [17] for recent results in a waveguide geometry in the setting (a0), the existence theory for the medium is not affected by the compact perturbation. Similarly, existence theory for a waveguide geometry as in (b) was performed in [25].

Spectral analysis. We refrain from listing introductory literature, we only mention [10] and [21] for results on the existence of band gaps in purely periodic media. A spectral analysis in the case (a0) was performed in [8]: a compact perturbation of the medium generates defect modes, discrete eigenvalues that emerge from the continuous spectrum. Related is the emergence of eigenmodes in a gap, shown in [9] for strong enough defects of type (a0). A constant medium in the setting (a0) was analyzed in [13], the perturbation creates an embedded eigenvalue.

A medium with a line defect (a1) was analyzed in [4] with interesting general methods. It is shown that the perturbation of the medium along a line introduces additional spectrum in spectral gaps of the periodic medium. The methods were extended in [16] to show the creation of additional spectrum in the case (a2), and for more general systems of equations, including Maxwell's equations.

A problem of type (b) was treated in [22], and we actually use a very similar geometry. We mention that the paper introduces some unsatisfactory assumptions in the course of the analysis. A one-dimensional investigation of the bulk-edge correspondance related to our waveguide geometry can be found in [20].

Topological methods. Even though our approach was inspired by such theories, we do not use topological methods. The field is fascinating, it is related to the quantum-Hall effect and was growing quickly since its discovery in the 1980ies. Roughly speaking, one can associate a topological invariant to a periodic medium and one can show by quite general methods that, at the interface between two topologically different media (one can be vacuum), there are always edge-states. These are stable under perturbations since they are "topologically protected". The spectrum of the combined medium (e.g.: periodic medium plus interface plus vacuum) is different from the spectrum of the two periodic media. This “bulk-edge correspondance” was probably observed firstly in [15]. Oftentimes, one uses for the analysis discrete systems; a prominent example is the simple and yet rich SSH-model of [26]. For a full proof of a satisfactory result in this direction we refer to [5]: Using periodic media of different topological properties on the two sides of an interface necessarily generates edge states by a formula that relates different mathematical degrees. Closer to our approach is [7], where the indices for small perturbations of elliptic operators are calculated, also with the result that interface modes occur, see also [2, 6, 19].

An extension to photonic crystals was performed in the language of physics in [23] and [14], where edge-states for topological insulators for Maxwell’s equations were found. Bulk-edge correspondance in two space dimensions is also the topic of the more mathematically inclined paper [12], where different topological bulk- and edge-indices are introduced and related. Methods are inspired by [24].

2 Example geometry, Dirac point, gap opening

This section is devoted to the description of a geometry for which Assumption 1.1 holds. It shows the Dirac point in the unperturbed medium, the gap opening in the perturbed medium, the differentiability of Definition 2.1 and $B^I = -B^{II}$. We use this geometry in our numerical experiments.

2.1 Geometry: Construction and assumptions

The construction was already sketched in Subsection 1.1, it is illustrated in Figure 3. The left image shows the $(0, 1/2) \times \Sigma$ periodicity cell for b_0. In the middle, we see the same geometry, now considered as a 1-periodic medium with the periodicity cell $(0, 1) \times \Sigma$. The right image shows the perturbed 1-periodicity cell of Medium I. It is constucted by moving the inclusions slightly away from the mid-line $x_1 = 1/2$.

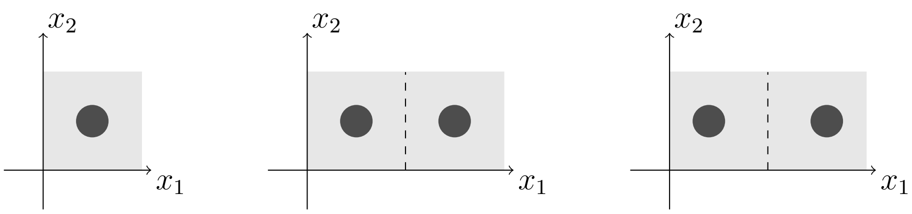

Figure 3: Left: The cell $(0, 1/2) \times \Sigma$ corresponding to media with 1/2-periodicity. Middle: The same medium, now regarded as 1-periodic with the periodicity cell $(0, 1) \times \Sigma$. Right: A perturbation of the 1-periodic medium cell leads to a 1-periodic medium that is no longer 1/2-periodic.

For numerical experiments, we use the dimension $d = 2$ and the cross-sectional domain $\Sigma = (0, 1/2) \subset \mathbb{R}^{d-1}$ such that $\Omega = \mathbb{R} \times (0, 1/2)$. We use $a \equiv a_0 \equiv 1$ and, everywhere except for the inclusions, $b = 1$ and $b_0 = 1$. The centers of inclusions are at points $(x_1, 1/4)$ with $x_1 = \ell + 1/2 - r_0$ and $x_1 = \ell + 1/2 + r_0$ for $\ell \in \mathbb{Z}$. The 1/2-periodic medium is generated with $r_0 = 0.25$. We choose $r_0 = 0.25 + 0.03$ for Medium I and $r_0 = 0.25 - 0.03$ for Medium II.

In elliptical regions around these centers, the parameter b is varied. We define, for $\xi \in \mathbb{R}^2$, a norm by setting $\|\xi\|_E^2 := |\xi_1 + \xi_2|^2/2 + 2\,|\xi_1 - \xi_2|^2$. An elliptic region with center x is defined by $\{y \in \mathbb{R}^2 | \|y - x\|_E^2 < \delta^2\}$, we choose in all experiments $\delta = 1/18$. The parameters b and b_0 are set to 1 everywhere except for the regions around the various centers. When y is a point close to a center x, more precisely, when $\|y - x\|_E < 0.4\,\delta$, we set $b(y) = 21$. To have a continuous transition, we set $b(y) = 1 + 20\,(1 - \|y - x\|_E/\delta)/0.6$ in the remaining elliptical ring. The parameter b is illustrated in Figure 4. The small parameter ε is the shift of the b-inclusions; in this sense, our numerical experiments use $\varepsilon = 0.03$.

For the rigorous analysis, we need abstract properties of the coefficients. Let us collect properties of the coefficients that are studied in this contribution. We use the 1-periodicity cell $Y = (0, 1) \times \Sigma$ and the (left) 1/2-periodicity cell $Y_{1/2} := (0, 1/2) \times \Sigma$.

Regarding the subsequent definition, we recall that we demand the differentiability property separately for Medium I and Medium II.

Definition 2.1 (Differentiability with respect to ε)**.** *For all $\varepsilon > 0$ we assume that b_ε is 1-periodic. We demand the following differentiability: For some $B \in L^2(Y, \mathbb{R})$, in the limit $\varepsilon \to 0$, there holds*

$$\frac{b_\varepsilon - b_0}{\varepsilon} \to B \quad \text{in} \quad L^2(Y, \mathbb{R})\,. \tag{2.1}$$

For notational convenience, we consider no perturbations in the other coefficient and demand $a_\varepsilon = a_0$. We additionally assume that a_0 is a constant function.

We note that the differentiability property is satisfied when b_0 is of class $H^1(Y)$ and the coefficients b_ε are defined by shifts as described above. Obviously, it is also satisfied for coefficients such as $b_\varepsilon = b_0 + \varepsilon b_1$ with an L^2-function b_1.

We assume $B^I = -B^{II}$ in our main result. Loosely speaking, this means that Medium II is obtained in the same way as Medium I, but perturbing in the opposite direction. It is satisfied when some family b^0_ε is constructed for $\varepsilon \in (-\varepsilon_1, \varepsilon_1)$ and one chooses, for $\varepsilon > 0$, the media $b^I_\varepsilon = b^0_\varepsilon$ and $b^{II}_\varepsilon = b^0_{-\varepsilon}$.

Assumption 2.2 (Symmetry assumptions)**.** *Several symmetry assumptions can be considered for media as in Definition 2.1.*

(i) The shift anti-symmetry $B(1/2 + x_1, \tilde{x}) = -B(x_1, \tilde{x})$ for almost all $(x_1, \tilde{x})$ with $x_1 < 1/2$. Loosely speaking: The second half-cell is treated exactly as the first half-cell, but in opposite direction. When (i) holds and the two media satisfy $B^I = -B^{II}$, then the two media coincide up to a shift by 1/2 (at least on the level of derivatives).

(ii) Reflection symmetry: For every ε under consideration, the function b_ε is symmetric in the sense that

$$b_\varepsilon(1 - x_1, \tilde{x}) = b_\varepsilon(x_1, \tilde{x}) \quad \text{for almost every } (x_1, \tilde{x}) \in Y\,. \tag{2.2}$$

In particular, the linearization is also symmetric, $B(e_1 - \cdot) = B(\cdot)$.

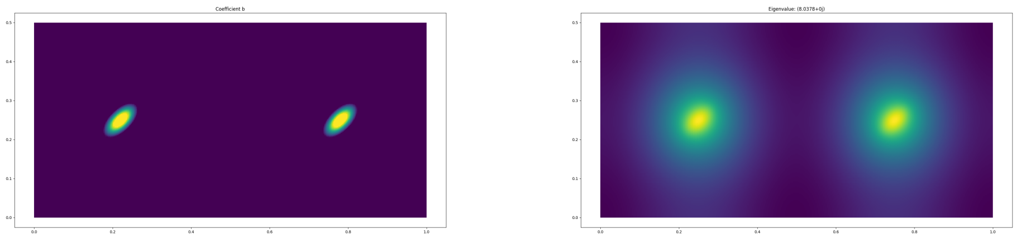

Figure 4: Left: The coefficient b in the numerical realization for the perturbed problem. We violate the symmetry assumption (ii) by using tilted ellipses. Right: The first eigenfunction for the unperturbed problem, the eigenvalue is $\lambda_* = 8.038$. Plotted is the periodic function as it is obtained by performing numerical calculations in the space of periodic functions.

2.2 The unperturbed medium, basis functions V and W

Our next aim is to construct two fundamental functions V and W that are used in our proofs. In the course of our constructions, we will also see why the 1/2-periodic medium typically exhibits, when considered as a 1-periodic medium, a Dirac point.

Given a cross-sectional domain $\Sigma \in \mathbb{R}^{d-1}$, we introduce the positive number $\sigma := 1/\sqrt{|\Sigma|}$ with the property $\int_\Sigma \sigma^2 = 1$.

Half-cell problem and the family U

For a wave-parameter k, the problem of finding quasiperiodic solutions in the half-cell $Y_{1/2} = (0, 1/2) \times \Sigma$ is the following: Find $U : Y_{1/2} \to \mathbb{C}$ solving

$$-\nabla \cdot (a_0 \nabla U) = \lambda\, b_0\, U \qquad \text{in } Y_{1/2}\,, \tag{2.3}$$

$$U|_{x_1=1/2} = e^{ik/2} U|_{x_1=0}\,, \quad \partial_1 U|_{x_1=1/2} = e^{ik/2} \partial_1 U|_{x_1=0}\,. \tag{2.4}$$

Any solution U can be extended to a solution on the 1-cell $Y = (0,1) \times \Sigma$ by setting $U(x_1, \tilde{x}; k) = e^{ik/2} U(x_1 - 1/2, \tilde{x}; k)$ for $x_1 > 1/2$. We normalize U such that the extended function satisfies $\int_Y b_0 |U|^2 = 1$. This normalization still allows for phase-factors. We always demand that U is chosen so that the integral $\int_\Sigma U(0, \cdot; k)$ is real with non-negative real part. To simplify the discussion below, we assume that the value $\int_\Sigma U(0, \cdot; k)$ is not vanishing; otherwise, one must use a different normalization, e.g., using only a subset of Σ. Multiplication of (2.3) with $\bar{U}$ and an integration over $Y_{1/2}$, exploiting the quasi-periodicity, yields $\int_Y a_0 |\nabla U|^2 = \lambda$.

The normalizations are chosen so that, for $a_0 \equiv 1$ and $b_0 \equiv 1$, the eigenfunction for the smallest eigenvalue is $U(x; k) = \sigma e^{ikx_1}$ and the eigenvalue is k^2.

For every $k \in [0, 2\pi]$, we find a countable sequence of eigenvalues λ, i.e., real numbers such that problem (2.3)–(2.4) has a non-trivial solution U. We denote these eigenvalues with $j \in \mathbb{N}$ as $\mu_j(k)$, the curves $k \mapsto \mu_j(k)$ are the dispersion curves, the first three dispersion curves for the half-cell problem are shown in the left part of Figure 6. The typical choice is to consider the family $U = U(x, k)$ of solutions for the smallest eigenvalue $\mu_0(k)$; our analysis allows also to choose another branch μ_j, we only require that, for every k near $k_0 = \pi$, the solution space of (2.3)–(2.4) with $\lambda = \mu_j(k)$ is one-dimensional.

Full-cell problem, basis functions V and W

We next want to regard the unperturbed coefficients as a 1-periodic medium, see Figure 5. The reason is that we will consider perturbations within the class of 1-periodic media. The unperturbed problem in the full-cell $Y = (0,1) \times \Sigma$ is: Find $\Phi : Y \to \mathbb{C}$ solving

$$-\nabla \cdot (a_0 \nabla \Phi) = \lambda\, b_0\, \Phi \qquad \text{in } (0,1)\times\Sigma\,, \tag{2.5}$$

$$\Phi|_{x_1=1} = e^{ik}\Phi|_{x_1=0}\,, \quad \partial_1\Phi|_{x_1=1} = e^{ik}\partial_1\Phi|_{x_1=0}\,. \tag{2.6}$$

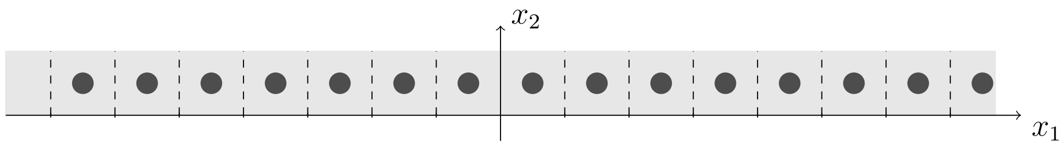

Figure 5: Sketch of the unperturbed periodic medium in dimension $d = 2$, it is 1/2-periodic. Considered as a 1-periodic medium, its dispersion curves typically have a Dirac point at $k = \pi$.

We can construct, for every $k \in [0, 2\pi]$, two solutions to this problem. The first is $U(\,\cdot\,;k)$; we recall that we have extended U to all $x_1 \in (0,1)$ and that, for $a_0 \equiv b_0 \equiv 1$, there holds $U(x;k) = \sigma e^{ikx_1}$.

Another solution can be found by reflecting the wave-parameter k across $k = \pi$ and by using a complex conjugation: We set $\tilde U(\,\cdot\,;k) := \overline{U(\,\cdot\,;2\pi - k)}$. Indeed, regarding the values at the two sides, we can calculate

$$\tilde U((1,\tilde x);k) = \overline{U((1,\tilde x);2\pi-k)} = \overline{e^{i(2\pi-k)}U((0,\tilde x);2\pi-k)} = e^{ik}\tilde U((0,\tilde x);k)\,.$$

Likewise, we also obtain the quasi-periodicity of derivatives:

$$\partial_1\tilde U((1,\tilde x);k) = \overline{e^{i(2\pi-k)}\partial_1 U((0,\tilde x);2\pi-k)} = e^{ik}\partial_1\tilde U((0,\tilde x);k)\,.$$

This shows that every eigenvalue occurs twice in the 1-periodicity cell: As an eigenvalue for k and as an eigenvalue for $2\pi - k$. This can be seen in Figure 6: The three curves of the left image appear twice in the right image, once in their original form and once reflected across $k = \pi$.

We assume that the first dispersion curve of the 1/2-cell, $k \mapsto \mu_0(k)$, is monotonically increasing in the vicinity of $k = \pi$. In this case, for every $k \neq \pi$, the two functions $U(\,\cdot\,;k)$ and $\tilde U(\,\cdot\,;k)$ are orthogonal in the b_0-scalar product by the standard calculation

$$\begin{aligned}\mu_0(k)\int_Y b_0(x)U(x;k)\overline{\tilde U(x;k)}\,dx &= \int_Y a_0(x)\nabla U(x;k)\nabla\overline{\tilde U(x;k)}\,dx\\ &= \mu_0(2\pi-k)\int_Y b_0(x)U(x;k)\overline{\tilde U(x;k)}\,dx\,,\end{aligned}$$

and the observation that $\mu_0(k) \neq \mu_0(2\pi - k)$ for $k \neq \pi$. When the two families U and $\tilde U$ are chosen as continuous functions in k, then they are also orthogonal for $k = \pi$ by continuity.

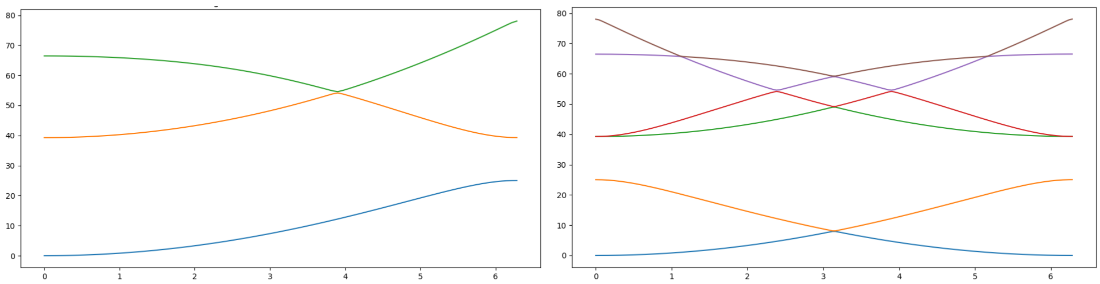

Figure 6: The eigenvalue bands, the first coordinate is $k \in [0, 2\pi]$, the second coordinate is for the eigenvalue $\lambda \in [0, 80]$. Left: The 1/2-periodicity cell. For every $k \in [0, 2\pi]$, the first three eigenfunctions with quasiperiodicity k are plotted. Right: The 1-periodicity cell. Every band of the left image occurs twice, once in a reflected version, mirrored at $k = \pi$.

This concludes the construction of the two b_0-orthogonal basis functions V and W that are of utmost importance throughout this text. We set

$$V := U(\,\cdot\,;\pi) \qquad \text{and} \qquad W := \tilde{U}(\,\cdot\,;\pi) = \bar{V}\,. \tag{2.7}$$

We emphasize that they are defined for the unperturbed problem and for the special parameter $k = \pi$. They are uniquely determined (possibly up to a phase factor). When the coefficients a and b are close to constants, we can expect $V(x) \approx \sigma\, e^{i\pi x_1}$ and $W(x) \approx \sigma\, e^{-i\pi x_1}$.

Let us collect further properties. We always identify the functions with their quasiperiodic extensions, these solve $-\nabla \cdot (a_0\, \nabla V) = \lambda_0\, b_0\, V$ in Ω. They satisfy the normalizations and orthogonalities

$$\int_Y a_0 |\nabla V|^2 = \int_Y \lambda_0 b_0 |V|^2 = \lambda_0\,, \tag{2.8}$$

$$\int_Y a_0 \nabla W \cdot \nabla \bar{V} = \int_Y \lambda_0 b_0 W \bar{V} = 0\,, \tag{2.9}$$

where the normalization (2.8) is also valid for W. By their construction from U, we have the quasiperiodicities $V(\cdot + e_1/2) = iV(\cdot)$ and $W(\cdot + e_1/2) = -iW(\cdot)$. In particular, the squared functions satisfy $V^2(\cdot + e_1/2) = -V^2(\cdot)$ and the absolute value functions $|V|$ and $|W|$ are both 1/2-periodic.

Symmetric media. Let us consider the case that the unperturbed medium has a reflection symmetry in the sense that $a_0(1 - x_1, \tilde{x}) = a_0(x_1, \tilde{x})$ and $b_0(1 - x_1, \tilde{x}) = b_0(x_1, \tilde{x})$ for all $x_1 \in [0, 1]$ and $\tilde{x} \in \Sigma$. We note that we always assume the 1/2-periodicity of the unperturbed coefficients, hence we also find $a_0(1/2 - x_1, \tilde{x}) = a_0(1 - x_1, \tilde{x}) = a_0(x_1, \tilde{x})$, and likewise for b_0. In this case, the function $\Psi : (x_1, \tilde{x}) \mapsto U(1/2 - x_1, \tilde{x}; \pi)$ is a solution of (2.3) with $\Psi|_{x_1=1/2} = U(\cdot;\pi)|_{x_1=0} = -iU(\cdot;\pi)|_{x_1=1/2} = -i\Psi|_{x_1=0}$, and likewise for the derivative. Since we assumed that solutions of (2.3)–(2.4) are unique up to complex factors, Ψ must coincide with a multiple of $\bar{V} = \bar{U}(\cdot;\pi)$. Since Ψ is normalized, the pre-factor can only be a phase shift. We have obtained that, in symmetric media, for some $\eta \in \mathbb{C}$ with $|\eta| = 1$, we have the additional relation

$$V(1 - x_1, \tilde{x}) = i\; V(1/2 - x_1, \tilde{x}) = \eta \bar{V}(x_1, \tilde{x}) \quad \forall x_1 \in [0, 1]\,,\;\; \tilde{x} \in \Sigma\,. \tag{2.10}$$

In particular, $|V(1-x_1,\tilde{x})| = |V(x_1,\tilde{x})|$ for all $(x_1,\tilde{x})$. The absolute value functions $|V|$ and $|W|$ are not only 1/2-periodic, but have also the reflection symmetry.

We recall that we have chosen the normalization that $\fint_\Sigma V(0,\cdot)$ is real with positive real part (possibly also for a subset of Σ, this does not change the subsequent argument). Since $V(1,\cdot) = -V(0,\cdot)$, setting $x_1 = 1$ in (2.10) and integrating over Σ, we obtain that $\fint_\Sigma V(0,\cdot) = \eta \fint_\Sigma \bar{V}(1,\cdot) = -\eta \fint_\Sigma \bar{V}(0,\cdot)$. Both integrals are real and positive, we can therefore conclude $\eta = -1$. This provides, for symmetric media, $V(1-x_1,\tilde{x}) = -\bar{V}(x_1,\tilde{x})$ and $V^2(1-x_1,\tilde{x}) = \bar{V}^2(x_1,\tilde{x})$.

2.3 Flux and gap opening

We have already seen that a Dirac point occurs in $k=\pi$; it is a result of superimposing a monotone curve with its reflected version, see Figure 6. An image of a corresponding eigenfunction is plotted in the right part of Figure 4; we plot a periodic function as it is obtained in our numerical code. To obtain the physically relevant quasiperiodic eigenfunction V, one must multiply with $e^{i\pi x_1}$, compare the left part of Figure 7.

To the function V we can associate a flux quantity. With the unit cell $Y = (0,1)\times\Sigma$, we set

$$F_{\mathbb{C}} := \int_Y a\bar{V}\,\partial_1 V\,, \qquad F := -iF_{\mathbb{C}}\,. \tag{2.11}$$

For a constant coefficient function a, the complex flux $F_{\mathbb{C}}$ is purely imaginary: Indeed, the 1-quasiperiodicity of $|V|^2$ allows to calculate $0 = \fint_Y \partial_1(a|V|^2) = \operatorname{Re}\fint_Y aV\,\partial_1\bar{V} = \operatorname{Re} F_{\mathbb{C}}$. We can therefore write $F_{\mathbb{C}} = iF$ with $F\in\mathbb{R}$. In our main result, we assume $F\neq 0$.

Remark 2.3 (Intuition)**.** *We have already seen that, for $a\equiv 1$ and for b approximately 1, with $\sigma>0$ chosen so that $\fint_\Sigma \sigma^2 = 1$, we expect $U(x;k)\approx \sigma\, e^{ikx_1}$ and $\tilde{U}(x;k)\approx \sigma\,\overline{e^{i(2\pi-k)x_1}} = \sigma\, e^{i(k-2\pi)x_1}$ for $x_1\in(0,1)$. For the special value $k=\pi$, the two functions are $V(x) = U(x;\pi)\approx \sigma e^{i\pi x_1}$ and $W(x) = \tilde{U}(x;\pi)\approx \sigma e^{-i\pi x_1}$. Within the same approximation, we expect $a\bar{V}\,\partial_1 V \approx \sigma^2 i\pi$ and hence $F_{\mathbb{C}}\approx i\pi$ and $F\approx\pi$.*

For $k<\pi$, the smallest eigenvalue corresponds to an eigenfunction that is close to V, for $k>\pi$, the smallest eigenvalue corresponds an eigenfunction close to W.

Perturbed medium and gap opening. The perturbed medium is 1-periodic, but it is not 1/2-periodic. The dispersion curves are modified, we observe that a gap is created in the lowest Dirac point with $k=\pi$. For a zoom into the first spectral gap see the right part of Figure 7; it shows the perturbation of the first crossing point in the right image of Figure 6. Numerically, we actually see that gaps form also in the Dirac points of the higher modes.

3 Reduced spatial dynamics

Our method is based on the study of inhomogeneous problems with particular right-hand sides. We are interested in the analysis of the perturbed inhomogeneous problem

$$-\nabla\cdot(a_\varepsilon\nabla u) - \lambda\, b_\varepsilon\, u \;=\; f\,. \tag{3.1}$$

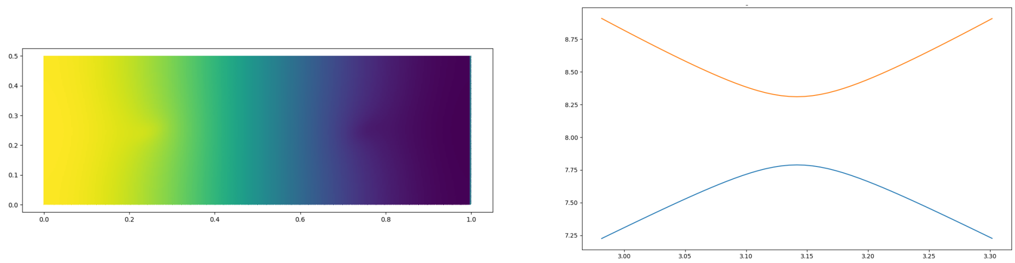

Figure 7: Left: The real part of the first π-quasiperiodic eigenfunction in the cell $(x_1, x_2) \in (0,1) \times (0,1/2)$. We see the mathematically relevant function V. It is close to (a multiple of) $\exp(i\pi x_1)$, indeed, the perturbation is hardly visible. Right: Zoom into the first spectral gap for the perturbed problem with $r_0 = 0.25 + 0.03$. The maximum of the lower curve is $\lambda_0 = 7.78$, the minimum of the upper curve is $\lambda_1 = 8.3$, the extrema are located at $k = \pi$. The gap-width is $\lambda_1 - \lambda_0 = 0.52$.

The right-hand side is constructed from the basis function V with an envelope function $g : \mathbb{R} \to \mathbb{C}$,

$$f(x) := V(x) g(x_1)\,. \tag{3.2}$$

We recall that the basis function V is expected to have similarity with $x \mapsto e^{i\pi x_1}$ on the 1-periodicity cell (more precisely: for constant coefficients a and b, the function $V(x)$ is a multiple of the function $\sigma e^{i\pi x_1}$).

We will assume that variations of g happen on a scale that is large (large compared to the periodicity, which is 1). One may think of a Gaussian localization function, $g(x_1) = \exp(-x_1^2/s^2)$ with large $s \in \mathbb{R}_+$. Another choice is a characteristic function, $g(x_1) = \mathbf{1}_{(-s,s)}(x_1)$ with large $s \in \mathbb{R}_+$. This is actually the function that we use in the numerics. We always consider $\lambda > 0$ in the spectral gap.

The underlying idea of the reduced dynamics is that, when λ is in the spectral gap and the spectral gap is narrow, then the solution u is necessarily, up to a small error, a linear combination of the two eigenfunctions with eigenvalue close to λ. This is formalized with the ansatz

$$u(x) = \alpha(x_1) V(x) + \beta(x_1) W(x) + \tilde{u}(x)\,, \tag{3.3}$$

and the assumption that $\tilde{u}$ is small.

We will derive a reduced system of ordinary differential equations for the coefficients $\alpha, \beta : \mathbb{R} \to \mathbb{C}$. For parameters $A, p \in \mathbb{R}$ and $q \in \mathbb{C}$, we find the system

$$\alpha' = ip\alpha + iq\beta + iAg\,, \tag{3.4}$$
$$\beta' = -ip\beta - i\bar{q}\alpha\,. \tag{3.5}$$

The parameters p and q depend on the medium. Under symmetry assumptions holds: p is the same parameter for both media. When $q = q_0$ is the parameter for Medium I, then the parameter $q = -q_0$ must be used for Medium II.

In this section, we give a formal derivation of (3.4)–(3.5). In Section 5, we make the derivation rigorous within a homogenization setting.

Further description of numerical experiments. In most numerical experiments, we use 70 periodicity cells, 35 to the left and 35 to the right from $x_1 = 0$. We use finite elements with piecewise linear ansatz functions, we typically discretize each periodicity cell with a grid of 23×23 points. As function g we use $g(x_1) = \mathbf{1}_{(-s,s)}(x_1)$ with $s = 15$. The media are defined with the positional values $r_0 = 0.25 \pm 0.03$, i.e., $\varepsilon = 0.03$. We recall that the typical size of the inclusions is given by $\delta = 1/18$. The spectral parameter is $\lambda \in (7.8, 8.3)$. The function V is calculated with finite elements on the 1-cell Y.

We observe a remarkable agreement of the reduced dynamics with the projections of the solution u to (3.1). For the fixed geometry described above, we always used $q = 0.045$ for Medium I and, accordingly $q = -0.045$ for Medium II. The parameter p varies with the value of λ, it is of the same order as q. Let us describe how we generated the graphs in Figures 8, 9 and 11. In all figures on the left is a result of the following procedure: For some value of λ, the finite element code provides an approximate solution u to the two-dimensional problem (3.1) with the chosen right-hand side f. We plot, for integers $r \in (-35, 34)$ and the cells $Q_r = (r, r+1) \times (0, 1/2)$, the real and imaginary parts of the integrals $\alpha_{\text{num}}(r) = \int_{Q_r} u\bar{V}$ and $\beta_{\text{num}}(r) = \int_{Q_r} u\bar{W}$. In all figures on the right, we plot real and imaginary parts of the solutions (α, β) of (3.4)–(3.5) with the boundary conditions $\alpha = \beta$ in $x_1 = \pm 35$. All figures show a remarkable agreement for these two methods of calculating the coefficients α and β.

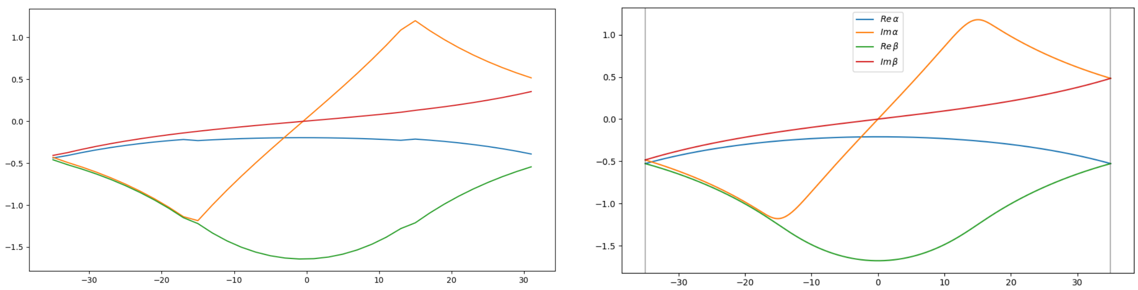

Figure 8: Factors α and β for Medium I, $r_0 = 0.25 + 0.03$. Left: A two-dimensional calculation for $\lambda = 8.07$. For the solution u of (3.1) we plot, for integers $r \in (-35, 35)$ on the horizontal axis, the real and imaginary parts of the integrals $\alpha_{\text{num}}(r) = \int_{Q_r} u\bar{V}$ and $\beta_{\text{num}}(r) = \int_{Q_r} u\bar{W}$. The curve with the highest maximum is $\text{Im}(\alpha)$, the curve with the lowest minimum is $\text{Re}(\beta)$, the monotonically increasing curve is $\text{Im}(\beta)$. Right: Solutions of (3.4)–(3.5) with $A = 1/(2\pi)$, $p = 0$ and $q = 0.045$.

A formal derivation of reduced spatial dynamics

Our aim here is give a short formal derivation of the reduced dynamics. We write a and b instead of a_ε and b_ε to have better readable formulas. We consider an arbitrary differentiable function $\psi : \mathbb{R} \to \mathbb{R}$ with compact support that we use as an envelope function. We multiply (3.1) with $\psi(x_1)\bar{V}(x)$ and integrate over Ω to find

$$\int_\Omega a\nabla u \cdot \nabla(\psi\bar{V}) - \lambda \int_\Omega b\, u\, (\psi\bar{V}) - \int_\Omega g\psi\, V\bar{V} = 0\,.$$

We insert the ansatz (3.3). Moving terms involving $\tilde{u}$ to the right hand side, we have

$$\int_\Omega a\nabla(\alpha V + \beta W) \cdot \nabla(\psi\bar{V}) - \lambda \int_\Omega b(\alpha V + \beta W)\, (\psi\bar{V}) - \int_\Omega g\psi\, V\bar{V} = F_1\,, \tag{3.6}$$

with

$$F_1 := -\int_\Omega a\nabla\tilde{u}\cdot\nabla(\psi\bar{V}) + \lambda\int_\Omega b\,\tilde{u}\,(\psi\bar{V})\,.$$

Later on, we will neglect "error terms" F; the function F_1 is small when $\tilde{u}$ of the ansatz (3.3) is small. We turn our attention to the left-hand side of (3.6). The gradients in the first integral can be evaluated with the product rule and we obtain

$$\begin{aligned}
&\int_\Omega a\left\{\alpha\psi|\nabla V|^2 + \beta\psi(\nabla W\cdot\nabla\bar{V})\right\}\\
&\quad + \int_\Omega a\left\{\alpha'\psi V\partial_1\bar{V} + \alpha\psi'\partial_1 V\bar{V} + \beta'\psi W\partial_1\bar{V} + \beta\psi'\partial_1 W\bar{V}\right\}\\
&\quad + \int_\Omega a\left\{\alpha'\psi'|V|^2 + \beta'\psi' W\bar{V}\right\}\\
&\quad - \lambda\int_\Omega\left\{b\alpha\psi|V|^2 + b\beta\psi W\bar{V}\right\} - \int_\Omega g\psi\,|V|^2 = F_1\,.
\end{aligned}$$

In our next simplification step we assume that α, β and ψ depend slowly on x_1. This allows to neglect the third line since it contains products of derivatives of these functions.

In order to proceed further, we need some notation: For every position $r\in\mathbb{R}$ in the waveguide, the neighboring segment of the waveguide is denoted as $Q_r := (r, r+1)\times\Sigma$.

We recall the normalizations (2.8) of V and W and the orthogonalities (2.9). When we use these normalizations to evaluate integrals in the above expression, we introduce an error since, e.g., α is not constant in the single periodicity cell. Since variations of α are assumed to be small, the errors are small, we collect all errors in F_2. Note that we use here that $a = a_\varepsilon$ actually coincides with a_0. With this idea we replace, e.g., $\int_{Q_r} a|\nabla V|^2$ by $\lambda_0\int_{Q_r} b_0|V|^2$ in the first line. The second line is not changed. We obtain

$$\begin{aligned}
&\int_\Omega a\left\{\alpha'\psi V\partial_1\bar{V} + \alpha\psi'\partial_1 V\bar{V} + \beta'\psi W\partial_1\bar{V} + \beta\psi'\partial_1 W\bar{V}\right\}\\
&\qquad + \int_\Omega(\lambda_0 b_0 - \lambda b)\left\{\alpha\psi|V|^2 + \beta\psi W\bar{V}\right\} - \int_\Omega g\psi\,|V|^2 = F_1 + F_2\,.
\end{aligned}$$

Regarding the first line, we recall that cell-integrals over $aV\partial_1\bar{V}$ are $-iF$ (approximately $-i\pi$), and integrals over $a\bar{V}\partial_1 V$ are iF, see (2.11). In the other two terms: $aW\partial_1\bar{V}$ is vanishing, we show this in Appendix A. Let us mention that this is to be expected from the fact that this term is approximately $2e^{-i\pi x_1}(-i\pi)e^{-i\pi x_1} = -2i\pi e^{-2i\pi x_1}$, and hence highly oscillating. Likewise, the integral containing $\partial_1 W\bar{V}$ is vanishing. Since we neglect the (small) variations of the pre-factors (such as $\alpha\psi'$), we introduce errors; these are collected in a function F_3. We arrive at

$$\begin{aligned}
&\int_\mathbb{R}\{\alpha'\psi(-iF) + \alpha\psi'(iF)\}\\
&\qquad + \int_\Omega(\lambda_0 b_0 - \lambda b)\left\{\alpha\psi|V|^2 + \beta\psi W\bar{V}\right\} - \int_\Omega g\psi\,|V|^2 = F_1 + F_2 + F_3\,.
\end{aligned}$$

We can integrate by parts in the first line since ψ has compact support. We find that the two terms in the first integral are identical.

We rewrite the second line with the Taylor approximation $\lambda b - \lambda_0 b_0 \approx (\lambda-\lambda_0)b_0 + \lambda_0(b - b_0)$. This introduces an error that we put in the error function F_4. It is small when we assume the smallness of $|\lambda - \lambda_0|$ and $\|b - b_0\|$, the latter in an appropriate norm. Using that V and W are orthonormal with respect to the b_0-scalar product, and using $m := \int_0^1 \int_\Sigma |V|^2$, we obtain

$$\int_{\mathbb{R}} (-2iF)\alpha'\psi - \int_{\mathbb{R}} (\lambda - \lambda_0)\alpha\psi - \int_\Omega \lambda_0(b - b_0) \left\{\alpha\psi|V|^2 + \beta\psi W\bar{V}\right\}$$
$$= \int_{\mathbb{R}} mg\psi + F_1 + F_2 + F_3 + F_4 \,.$$

From now on, we neglect the error terms F_1 to F_4. Since ψ was arbitrary, we can read off an equation for α. After a multiplication with $i/(2F)$, the equation reads, using $Y = (0, 1) \times \Sigma$,

$$\alpha' = \frac{i}{2F}(\lambda - \lambda_0)\alpha + \frac{i}{2F}\lambda_0 \int_Y (b - b_0) \left\{\alpha|V|^2 + \beta W\bar{V}\right\} + \frac{im}{2F} g \,.$$

We obtain (3.4) with the parameters $A = m/(2F)$,

$$p = \frac{1}{2F}(\lambda - \lambda_0) + \frac{\lambda_0}{2F} \int_Y (b - b_0)|V|^2 \,, \tag{3.7}$$

$$q = \frac{\lambda_0}{2F} \int_Y (b - b_0)W\bar{V} = \frac{\lambda_0}{2F} \int_Y bW\bar{V} \,, \tag{3.8}$$

where we used (2.9) in the last equality. The formula shows that the parameter p is real. Furthermore, when the Medium II uses the same perturbation for $b - b_0$, but with opposite sign, then q only changes its sign when we switch from Medium I to Medium II.

When b defines a symmetric medium in the sense of (ii) of Assumption 2.2, $b(1 - x_1, \tilde{x}) = b(x_1, \tilde{x})$, then $W = \bar{V}$ together with $V^2(1 - x_1, \tilde{x}) = \bar{V}^2(x_1, \tilde{x})$ implies that q is real. When b is a shift anti-symmetric perturbation in the sense that $(b - b_0)(1/2 + x_1, \tilde{x}) = -(b - b_0)(x_1, \tilde{x})$ for all $(x_1, \tilde{x})$, related to (i) of Assumption 2.2, the integral in (3.7) vanishes, since $|V|$ is 1/2-periodic; we then find $p = (\lambda - \lambda_0)/(2F)$.

Equation (3.5) for $\beta'(x_1)$ is obtained with a similar calculation. One now multiplies (3.1) with $\psi(x_1)\bar{W}(x)$ and integrates over Ω to derive

$$-2iF \int_{\mathbb{R}} \beta'\psi \approx -\int_{\mathbb{R}} (\lambda - \lambda_0)\beta\psi - \int_\Omega \lambda_0(b - b_0) \left\{\beta\psi|V|^2 - \alpha\psi W\bar{V}\right\} .$$

Numerical values of parameters in the reduced model. Let us make a rough estimate for q in our numerical experiments. The number $\delta = 1/18$ is the radius of the inclusion in an ellipsoidal norm, the area of the inclusion is of the order δ^2. The variation of b is chosen as 20, the shift in x_1-direction is chosen as $\varepsilon = 0.03$, we make the usual approximation $W\bar{V} \approx e^{-2\pi i x_1}$. This function has in $x_1 = 1/4$ the value $-i$ and the x_1-derivative $-2\pi i\,(-i) = -2\pi$. We therefore expect q to be of order $(\lambda_0/(2\pi)) \cdot 2\delta^2 \cdot 20 \cdot (2\pi) \cdot 0.03 = \lambda_0 \cdot 40\delta^2 \cdot 0.03 \approx 0.03$. Numerically, we observe that this rough calculation provides the right order for q; a good fit was actually obtained with the choice $q = 0.045$.

Let us perform a similar estimate for p. Assuming that $|V|^2$ is well-approximated with 1 (which is not clear in the vicinity of the inclusion), we expect that the second

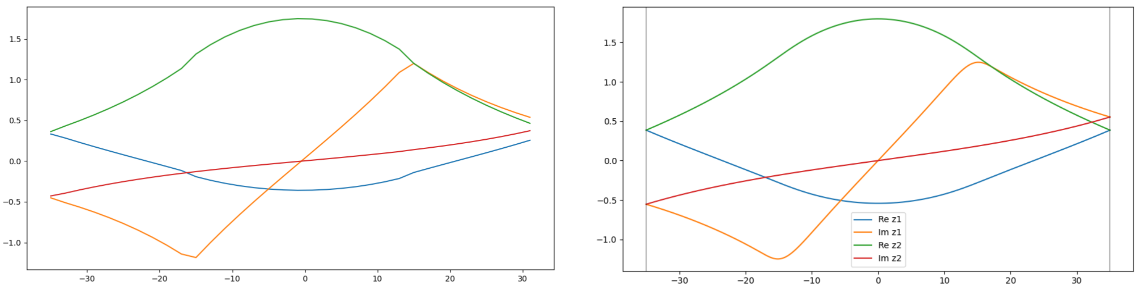

Figure 9: Reduced dynamics in Medium II, $r_0 = 0.25 - 0.03$, calculations as in Figure 8. Here, we use $\lambda = 7.98$, which is clearly below λ_0. Correspondingly, p is chosen negative in (3.4)–(3.5); we used $p = -0.02$ and $q = -0.045$. The curve for $\mathrm{Re}(\beta)$ is the curve with the highest maximum; in comparison with Figure 8 this curve is flipped to the upper part. This change is created by using Medium II instead of Medium I.

contribution to p is small. With $|\lambda - \lambda_0|$ having the order of 0.25 and with $2F$ being approximately 6, we expect for p values in the interval $(-0.04, 0.04)$. In particular: The orders of p and q are comparable (and of the order of ε).

We want to refer already here to the result of the subsequent Section 4. There, we derive that the critical values for p are essentially $\pm q_0$. The fact that p is comparable to q (which was derived above starting from formula (3.8)) fits well with the analysis of the reduced dynamics.

4 Analysis of the reduced dynamics

In this section, we analyze the system (3.4)–(3.5) for real parameters p and q. Classical methods provide the following properties.

Proposition 4.1 (Reduced dynamics)**.** *We consider the reduced system* (3.4)–(3.5) *on* $(-R, R)$ *with the boundary conditions* $\alpha = \beta$ *in* $x = \pm R$*. Let* $q_0 > 0$ *be a real number, we use below* $\rho_0 := \sqrt{q_0^2 + \pi^2/4R^2} > q_0$*. Medium I is modelled by setting* $q \equiv q_0$*, Medium II by setting* $q \equiv -q_0$*. The combined medium is modelled by setting* $q(x) = q_0$ *for* $x > 0$ *and* $q(x) = -q_0$ *for* $x < 0$*. The other coefficient is assumed to be constant, we use the parameter* $p \in \mathbb{R}$*.*

System (3.4)–(3.5) *has a non-trivial homogeneous solution in the following cases:*

(a) Medium I for parameters $p = -q_0$ *and* $p = \rho_0$*.*

(b) Medium II for parameters $p = -\rho_0$ *and* $p = q_0$*.*

(c) Combined medium for the parameter $p = 0$*.*

Let $g : (-R, R) \to \mathbb{R}$ *be a piecewise continuous function and let* $A > 0$ *be fixed. Then, the inhomogeneous problem* (3.4)–(3.5) *has a unique solution for Medium I and for Medium II when* p *is between the two critical values.*

Let g *additionally be a non-vanishing non-negative function. In all the three cases (a)–(c) holds: Solutions* (α, β) *of the inhomogeneous system are unbounded when* p *tends to one of the critical values. When* p *is a critical value, there does not exist a solution.*

The latter statement remains true for the unbounded domain: When g is non-vanishing and non-negative, for the combined medium and $p = 0$, there is no $L^2(\mathbb{R})$ solution (α, β) to the inhomogeneous system.

Proof. The system (3.4)–(3.5) is a linear boundary value problem for an ordinary differential equation. All statements can easily be checked using ansatz-functions of exponential type.

Critical parameters (a)–(c). The critical parameters for the single medium are calculated in Subsection 4.1. The critical parameters for the combined medium are calculated in Subsection 4.2.

Unique existence. Standard theory for linear boundary value problems yields that, when there is no nontrivial solution to the homogeneous problem, then there is a unique solution to the inhomogeneous problem. The calculations of Subsection 4.1 provide that there are only the given two values for p such that there exists a nontrivial solution to the homogeneous problem.

Vicinity of a critical value. The behavior of solutions when parameters approach the critical values is investigated in Subsection 4.3. □

On the interpretation of Proposition 4.1. The Helmholtz equation for the perturbed medium has a spectral gap around that Dirac-point spectral value λ_0. This implies that the operator corresponding to (1.1) is invertible for λ near λ_0. The counterpart for $\lambda - \lambda_0$ in the reduced system is p, the counterpart for the spectral gap is $p \in (-q_0, \rho_0)$ (for Medium I).

When λ approaches the edges of the spectral gap, the operator ceases to be invertible. This is reflected by the behavior of the reduced dynamics when p approaches one of the critical values.

The last statement of Proposition 4.1 is used in our proof of Theorem 1.2.

The numerical calculations shown in Figure 10 illustrate our results. Solutions of (3.4)–(3.5) become large when p is close to a critical parameter, the qualitative shape of solutions is as expected from the solutions of the homogeneous problems.

We note that the model predicts a different spectral gap for the two media. Nevertheless, the difference is only for finite R (on that level the media are different), the difference vanishes in the limit $R \to \infty$ (in this limit, the two media are undistinguishable). The limit interval is given by $-|q| =: p_0^\infty < 0 < p_1^\infty := |q|$.

4.1 The reduced dynamics in a single medium

We start with the case $q = q_0 > 0$. We write t for the independent variable x_1.

For the lower critical value $p = p_0 := -q$, a solution to the homogeneous version of (3.4)–(3.5) is easily found: We choose the constant functions $\alpha \equiv 1$ and $\beta \equiv 1$. The homogeneous system and the boundary conditions $\alpha(R) = \beta(R)$ and $\alpha(-R) = \beta(-R)$ are satisfied.

For the upper critical value $p = p_1 := \rho_0 = \sqrt{q^2 + \mu^2}$ with $\mu := \pi/(2R)$, the calculation is slightly longer. A solution can found with the ansatz

$$\alpha(t) = e^{i\mu t} + Be^{-i\mu t}\,, \tag{4.1}$$

$$\beta(t) = Ce^{i\mu t} + De^{-i\mu t}\,. \tag{4.2}$$

The choice of μ guarantees $e^{i\mu R} = i = -e^{-i\mu R}$. The boundary condition $\alpha = \beta$ in $t = R$ therefore reads $1 - B = C - D$. When we satisfy this condition, we have automatically also satisfied the boundary condition $\alpha = \beta$ in $t = -R$.

Equation (3.4) is satisfied when we achieve

$$i\mu = ip + iqC \quad \text{and} \quad -i\mu B = ipB + iqD\,. \tag{4.3}$$

The two equations are equivalent to $C = (\mu - p)/q$ and $D = -B\,(\mu + p)/q$. Equation (3.5) is satisfied when we achieve

$$i\mu C = -ipC - iq \quad \text{and} \quad -i\mu D = -ipD - iqB\,. \tag{4.4}$$

They are equivalent to $C = -q/(\mu + p)$ and $B = D\,(\mu - p)/q$.

We can therefore satisfy (4.3) and (4.4) simultaniously when the following two conditions are satisfied: (1) $(\mu - p)/q = -q/(\mu + p)$ or, equivalently, $p^2 - \mu^2 = q^2$. (2) $(\mu - p)/q = -q/(\mu + p)$. We observe that condition (2) is actually identical to condition (1).

In order to find the explicit solution, we calculate $1 - B = C - D = (\mu - p)/q + B\,(\mu + p)/q$. This condition yields $B\,(q + \mu + p) = q - \mu + p$ and hence a formula for B.

Let us collect our results: For the critical value $p = p_1$, the relation $p^2 - \mu^2 = q^2$ is satisfied and the homogeneous system has a non-trivial solution given by

$$B = \frac{q - \mu + p}{q + \mu + p}\,, \qquad C = (\mu - p)/q\,, \qquad D = -B\,(\mu + p)/q\,. \tag{4.5}$$

Medium II is modelled with $q = -q_0 < 0$, the above calculations remain valid and lead to the claim of (b). We note that $p = -q = q_0$ allows to choose constant functions as solutions of the homogeneous problem, this determines the larger critical value.

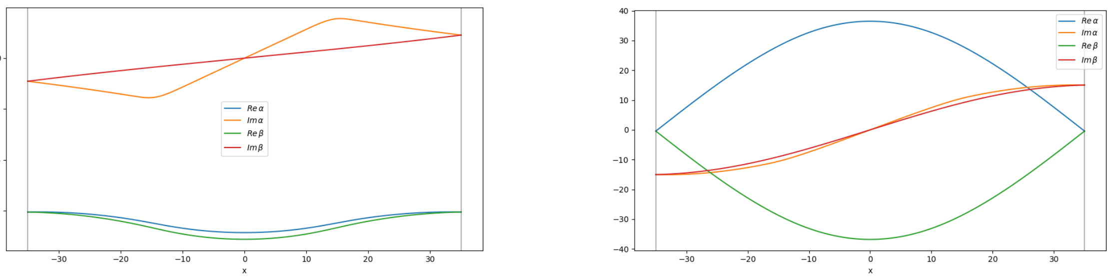

Figure 10: Large solutions of (3.4)–(3.5) in a single medium, described by $q = 0.045$, we choose p to model λ near the lower and upper end of the spectral gap. Left: $p = -q + 0.005$ is close to the lower critical value. Right: $p = \sqrt{q^2 + (3.0/(2R))^2}$ is close to the upper critical value.

4.2 The reduced dynamics for a combined medium

Using again $t = x_1 \in (-R, R)$ as independent variable and $q_0 > 0$, we now consider a coefficient $q = q(t)$ of the combined medium: $q(t) = q_0 > 0$ for $t > 0$ and

$q(t) = -q_0 < 0$ for $t < 0$. We claim that the homogeneous system (3.4)–(3.5) has a non-trivial solution for the parameter $p = 0$.

A solution of the homogeneous system can be found with the ansatz

$$\alpha(t) = ie^{qt} + Be^{-qt}\,, \quad \beta(t) = e^{qt} + iBe^{-qt}\,. \tag{4.6}$$

We note that we use the same formula for $t > 0$ and $t < 0$, exploiting the fact that q has a different sign in the two regions. The function is continuous in $t = 0$ with $\alpha(0) = i + B$ and $\beta(0) = 1 + iB$. The first equation is solved because of

$$iqe^{qt} - qBe^{-qt} = \alpha'(t) = iq\beta(t) = iqe^{qt} - qBe^{-qt}\,,$$

the second equation can be checked with the same calculation. It remains to satisfy the boundary conditions. Both boundary conditions $\alpha(\pm R) = \beta(\pm R)$ are satisfied when we achieve

$$ie^{q_0 R} + Be^{-q_0 R} = e^{q_0 R} + iBe^{-q_0 R}\,.$$

With the choice $B = e^{2q_0 R}$, we have found a non-trivial solution of the homogeneous system.

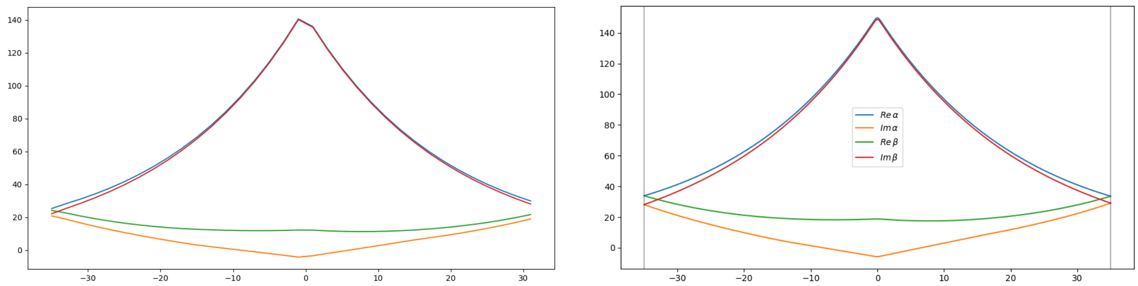

Figure 11: Solutions in the combined medium, Medium I for $x_1 > 0$ and Medium II for $x_1 < 0$. Left: 2D calculation for $\lambda = 8.05$. Right: System (3.4)–(3.5) with $q = 0.045$ for $x > 0$, $q = -0.045$ for $x < 0$ and $p = -0.0005$. We observe that the qualitative features of the solution are well predicted by the ansatz (4.6) with a large real constant B (the two functions with the high maximum in $t = 0$ are $\mathrm{Re}(\alpha)$ and $\mathrm{Im}(\beta)$).

When we consider the combined medium with $p = 0$ on the unbounded domain, we also find solutions. The functions

$$\alpha(t) = e^{-q(t)t} \quad \text{and} \quad \beta(t) = i\,e^{-q(t)t} \tag{4.7}$$

are non-trivial solution to the homogeneous system and of class $L^2(\mathbb{R})$.

4.3 The behavior when p approaches a critical parameter

Since this is the most interesting case for our subsequent analysis, we consider in detail the combined medium, i.e., $q = q(t)$ with $q(t) = q_0 > 0$ for $t > 0$ and $q(t) = -q_0 < 0$ for $t < 0$. Let (α, β) be a solution to the inhomogeneous problem (3.4)–(3.5) with $Ag \neq 0$ and for a parameter $p \in \mathbb{R}$. Let (α_0, β_0) be the solution to the homogeneous problem with vanishing parameter p; this solution has an explicit formula, see (4.6).

We multiply of (3.4) with $\bar\alpha_0$ and (3.5) with $\bar\beta_0$, integrate over $(-R,R)$ and subtract the results. We integrate by parts in the second equality. In the third equality we exploit homogeneous for (α_0,β_0) with vanishing parameter p to cancel four terms. The fourth equality exploits that the boundary terms vanish by our boundary condition.

$$\begin{aligned}\int_{-R}^{R} iAg\bar\alpha_0 &= \int_{-R}^{R}\left\{\alpha'\,\bar\alpha_0 - ip\alpha\bar\alpha_0 - iq\beta\bar\alpha_0 - \beta'\,\bar\beta_0 - ip\beta\bar\beta_0 - iq\alpha\bar\beta_0\right\}\\ &= \int_{-R}^{R}\left\{-\alpha\,\bar\alpha_0' + \alpha\,\overline{ip\alpha_0} + \beta\overline{iq\alpha_0} + \beta\,\bar\beta_0' + \beta\,\overline{ip\beta_0} + \alpha\,\overline{iq\beta_0}\right\}\\ &\quad + (\alpha\bar\alpha_0)|_{-R}^{R} - (\beta\bar\beta_0)|_{-R}^{R}\\ &= \int_{-R}^{R}\left\{\alpha\,\overline{ip\alpha_0} + \beta\,\overline{ip\beta_0}\right\} + (\alpha\bar\alpha_0)|_{-R}^{R} - (\alpha\bar\alpha_0)|_{-R}^{R}\\ &= p\int_{-R}^{R}\left\{\alpha\,\overline{i\alpha_0} + \beta\,\overline{i\beta_0}\right\}\,.\end{aligned}$$

The left hand side is independent of p and it is non-vanishing. Therefore, in the limit $p \to 0$, the solution sequence (α,β) must be unbounded. Furthermore, the calculation yields a contradiction for $p = 0$. This provides that there exists no solution of the inhomogeneous problem for $p = 0$.

The case $R = \infty$. For the combined medium on $\mathbb{R}$ we can perform the same calculation (without boundary terms), using the special homogeneous solution (α_0,β_0) of (4.7). We find the same properties of the system for $R = \infty$.

The homogeneous medium. The above calculation can also be used to show the claim in a single medium. We can exploit that, also for the single medium, there exist solutions of the homogeneous problem for which the real part has a single sign. We conclude the same properties: When p approaches the upper or the lower critical value, then solutions of the inhomogeneous problem (3.4)–(3.5) are necessarily diverging. When p is a critical value, no solution can exist.

5 Homogenization

In this section, we perform a rigorous derivation of the reduced dynamics. The mathematical derivation must use some limit procedure. With the small parameter $\varepsilon > 0$, we perform the following quite interesting limit: The perturbation of the medium is of order ε, in particular, for $\varepsilon = 0$, the medium is 1/2-periodic. This means that, in the limit $\varepsilon \to 0$, also the spectral gap closes. We are interested in an effect that is created by the perturbation, the open gap and the mismatch of the media and the eigenfunction at the interface – but our tool for the analysis is the limit procedure $\varepsilon \to 0$.

Let us include an analogy to the analysis of split ring resonators in Maxwell's equations that create negative index materials. The mathematical theory [3], is based on homogenization: For $\varepsilon > 0$, the rings have a slit of size ε, they are topologically trivial (simply connected domains). In the formal limit $\varepsilon = 0$, the rings are closed and topologically non-trivial (not simply connected). The topology allows for an interesting limit behavior, expressed by the existence of additional basis functions for $\varepsilon = 0$. This is analogous to our study of perturbed periodic media: In the formal limit $\varepsilon = 0$ with its additional symmetry, there exist basis functions V and W, they imply the interesting effect for $\varepsilon > 0$.

The parameter $\varepsilon > 0$ allows to distinguish between different scales. Variations of solutions and of basis functions V and W occur, in the original problem, on the spatial scale 1. We rescale the situation, $V(\cdot/\varepsilon)$ and $W(\cdot/\varepsilon)$ have variations on the spatial scale ε and envelope functions such as α, β, g or ψ will have variations in unit scales.

Let us now describe precisely the mathematical situation. We assume that a sequence $\varepsilon \to 0$ of positive numbers is fixed. For arbitrary numbers $r_\varepsilon > 0$ with positive lower bound, let I_ε be the intervals $I_\varepsilon := (-r_\varepsilon, r_\varepsilon)$. For the most part of our investigations, it is actually sufficient to think of a fixed interval, i.e., to have $r_\varepsilon = r$ independent of ε. A bounded Lipschitz domain $\Sigma \subset \mathbb{R}^{d-1}$ describes the cross-section of the waveguide, we write $Y := (0,1) \times \Sigma$ for the d-dimensional unit cell and $\Omega_\varepsilon := I_\varepsilon \times \varepsilon\Sigma$ for the rescaled domain. In the partial differential equation, we use the unperturbed coefficients $a_0(x/\varepsilon)$ and $b_0(x/\varepsilon)$, they are $\varepsilon/2$-periodic in x_1. The perturbed coefficients are $a_\varepsilon(x/\varepsilon)$ and $b_\varepsilon(x/\varepsilon)$. For notational convenience, we consider only the case $a_\varepsilon(y) = a_0(y)$ for all ε. Assumptions on the perturbed parameters b_ε are discussed below. For spectral parameters $\lambda_\varepsilon \to \lambda_0$ and right-hand sides f_ε, we are interested in the following equation on Ω_ε:

$$-\varepsilon^2 \nabla \cdot (a(x/\varepsilon)\nabla u^\varepsilon(x)) - \lambda_\varepsilon b_\varepsilon(x/\varepsilon) u^\varepsilon(x) = f_\varepsilon(x)\,, \tag{5.1}$$

where we impose homogeneous Neumann boudary conditions along all boundaries. We consider a special right-hand side: For a piecewise continuous function $g : \mathbb{R} \to \mathbb{C}$, we set

$$f_\varepsilon(x) := \varepsilon\, g(x_1) V(x/\varepsilon)\,. \tag{5.2}$$

Let u^ε be a sequence of solutions to (5.1). For the homogenization result, we assume that u^ε is bounded in the sense that

$$\frac{1}{\varepsilon^{d-1}} \int_{\Omega_\varepsilon} |u^\varepsilon|^2 \quad \text{is bounded.} \tag{5.3}$$

We note that this is a natural assumption for a function u^ε that has typical values of order 1 since the domain has the volume $|\Omega_\varepsilon| = 2r_\varepsilon\, \varepsilon^{d-1}\, |\Sigma|$.

When the intervals $I_\varepsilon = (-r_\varepsilon, r_\varepsilon)$ depend on ε, we assume $r_\varepsilon \in \varepsilon\mathbb{Z}$ and the convergence $r_\varepsilon \to r_* \in (0,\infty) \cup \{\infty\}$ and set $I = (-r_*, r_*)$.

We say that the sequence u^ε two-scale converges weakly in thin domains to the two-scale limit $u_0 : I \times Y_2 \to \mathbb{C}$ with $Y_2 := (0,2) \times \Sigma$ when, for every smooth test-function $\varphi = \varphi(x_1, y) : I \times Y_2 \to \mathbb{C}$ with compact support, there holds

$$\frac{1}{\varepsilon^{d-1}} \int_{\Omega_\varepsilon} u^\varepsilon(x)\varphi(x_1, x/\varepsilon)\, dx \to \frac{1}{2} \int_I \int_{Y_2} u_0(x_1, y)\varphi(x_1, y)\, dy\, dx_1\,. \tag{5.4}$$

The factor $1/2$ is necessary since the periodicity cell has the length 2; when all functions in the above expression are constant functions, we want to have $u_0 = u^\varepsilon$.

We can now formulate our main result on the limit process $\varepsilon \to 0$. It will be our tool to derive the existence of surface modes for small positive ε.

As before, we use F from (2.11) and assume $F \neq 0$, and set $A = m/(2F)$ with $m = \int_0^1 \int_\Sigma |V|^2$. The quantities $r_\varepsilon \to r_*$, I_ε and I are as described above.

Theorem 5.1 (Homogenization)**.** *Let $\lambda_0 > 0$ be a Dirac value for the medium (a_0, b_0) and let the pair (V, W) be an orthonormal basis of the corresponding eigenspace. Let $\lambda_\varepsilon \to \lambda_0$ be a sequence with $(\lambda_\varepsilon - \lambda_0)/\varepsilon \to \mu \in \mathbb{R}$. We consider the sequence u^ε of solutions to* (5.1) *with right-hand side f_ε of the form* (5.2) *for fixed $g : \mathbb{R} \to \mathbb{C}$, the domain is $\Omega_\varepsilon = I_\varepsilon \times \varepsilon\Sigma$. We assume that the sequence u^ε is bounded in the sense of* (5.3)*. Then, the following holds:*

1. *For a subsequence $\varepsilon \to 0$, there exists a two-scale limit $u_0 \in L^2(I \times Y_2, \mathbb{C})$ in the sense of* (5.4)*.*

2. *For two functions $\alpha, \beta : I \to \mathbb{C}$, the two-scale limit has the form*

$$u_0(x_1, y) = \alpha(x_1)V(y) + \beta(x_1)W(y) \quad \text{for a.e. } x_1 \in I\,,\ y \in Y_2\,. \tag{5.5}$$

3. *Let the coefficient functions b_ε be one of the following. (1) Every b_ε is periodic on the entire domain and thus modelling a single medium. It is a differentiable perturbation in the sense of Definition 2.1 with $B = \lim_{\varepsilon\to 0}(b_\varepsilon - b_0)/\varepsilon$. (2) There are periodic perturbed media b_ε^I and b_ε^{II} as above with derivatives B_I and B_{II}, b_ε is constructed by using b_ε^I for $x_1 > 0$ and b_ε^{II} for $x_1 < 0$. In this case, we set $B := B_I$ for $x_1 > 0$ and $B := B_{II}$ for $x_1 < 0$.*

   With this notation, the functions $\alpha, \beta \in L^2(I, \mathbb{C})$ satisfy, in the weak sense, the ordinary differential equations

$$\alpha' = ip\alpha + iq\beta + iAg\,, \tag{5.6}$$
$$\beta' = -ip\beta - i\bar{q}\alpha\,. \tag{5.7}$$

   The parameters are

$$p = \frac{1}{2F}\left(\mu + \lambda_0 \int_Y BV\bar{V}\right)\,, \tag{5.8}$$
$$q = \frac{1}{2F}\lambda_0 \int_Y BW\bar{V}\,. \tag{5.9}$$

4. *The parameters F and p are real. When b_ε satisfies the symmetric perturbation property (i) of Assumption 2.2, the formula for the first coefficient simplifies to $p = \mu/(2F)$. When b_ε satisfies the symmetric media property (ii) of Assumption 2.2 (for a combined medium: b_ε^+ and b_ε^- both satisfy this assumption) then q is real.*

   When the limit r_* is finite, then $\alpha, \beta : I \to \mathbb{C}$ satisfy the boundary conditions $\alpha(r_*) = \beta(r_*)$ and $\alpha(-r_*) = \beta(-r_*)$. In the case $r_* = \infty$ the boundary condition for the functions α and β is replaced by the requirement that both functions are of class $L^2(\mathbb{R}, \mathbb{C})$.

Proof. Item 1 follows from the classical general compactness result of L^2 with respect to weak two-scale convergence, see [1]. Here, we consider a thin domain. In order to apply the standard compactness result, one can concatenate copies of the solutions. Let us sketch the argument, for ease of notation we assume $\Sigma \subset (0,1)^{d-1}$. We construct a sequence of functions U^ε on the domain $\mathbb{R} \times (0,1)^{d-1}$ by setting, with the index set $\mathcal{K}_\varepsilon := \{k \in \mathbb{Z}^{d-1} | \varepsilon k \in (0,1)^{d-1}\}$,

$$U^\varepsilon(x_1, \tilde{x}) := \begin{cases} u^\varepsilon(x_1, \tilde{y}) & \text{if } \tilde{x} = \varepsilon(k + \tilde{y}) \text{ for some } k \in \mathcal{K}_\varepsilon\,,\ \tilde{y} \in \Sigma\,,\ |x_1| < r_\varepsilon\,, \\ 0 & \text{else.} \end{cases}$$

We extend U^ε trivially for $|x_1| \geq r_\varepsilon$. When u^ε satisfies the boundedness (5.3), then U^ε is a bounded sequence in $\mathbb{R} \times (0,1)^{d-1}$. Standard two-scale compactness can be applied to U^ε to find a subsequence and a weak two-scale limit function $U_0((x_1, \tilde{x}), (y_1, \tilde{y}))$ for $x = (x_1, \tilde{x}) \in \mathbb{R} \times (0,1)^{d-1}$ and $y = (y_1, \tilde{y}) \in Y_2$. Since U^ε is periodic in the directions $x_2, ..., x_d$, the function U_0 is independent of $\tilde{x}$. This yields $u_0(x_1, , (y_1, \tilde{y}))$ with the two-scale convergence property (5.4).

Item 2 is shown by deriving the equation that characterizes u_0. In the first parts of this proof, we consider an arbitrary test-function $\psi \in C_c^2(I)$ and a smooth periodic function $\phi : Y_2 \to \mathbb{C}$ that satisfies a Neumann condition along $(0,2) \times \partial\Sigma$. We use $\varphi_\varepsilon(x) := \psi(x_1)\phi(x/\varepsilon)$ as a test-function in (5.1). With two integrations by part, we obtain

$$\begin{aligned} &-\frac{1}{\varepsilon^{d-1}} \int_{\Omega_\varepsilon} u^\varepsilon(x)(\varepsilon^2 \nabla \cdot (a(x/\varepsilon)\nabla[\psi(x_1)\phi(x/\varepsilon)]))\, dx \\ &-\frac{1}{\varepsilon^{d-1}} \int_{\Omega_\varepsilon} u^\varepsilon(x)\lambda_\varepsilon b_\varepsilon(x/\varepsilon)\psi(x_1)\phi(x/\varepsilon)\, dx = \frac{1}{\varepsilon^{d-1}} \int_{\Omega_\varepsilon} f_\varepsilon(x)\psi(x_1)\phi(x/\varepsilon)\, dx\,. \end{aligned} \tag{5.10}$$

By definition of two-scale convergence, as $\varepsilon \to 0$, the three terms in this equation have the following limits:

$$\begin{aligned} &\frac{1}{\varepsilon^{d-1}} \int_{\Omega_\varepsilon} u^\varepsilon(x)(-\varepsilon^2 \nabla \cdot (a(x/\varepsilon)\nabla[\psi(x_1)\phi(x/\varepsilon)]))\, dx \\ &\qquad \to \frac{1}{2} \int_I \int_{Y_2} u_0(x_1, y)\psi(x_1)[-\nabla_y \cdot (a(y)\nabla_y \phi(y)]\, dy\, dx_1\,, \\ &\frac{1}{\varepsilon^{d-1}} \int_{\Omega_\varepsilon} u^\varepsilon(x)\lambda_\varepsilon b_\varepsilon(x/\varepsilon)\psi(x_1)\phi(x/\varepsilon)\, dx \\ &\qquad \to \frac{1}{2} \int_I \int_{Y_2} u_0(x_1, y)\lambda_0 b_0(y)\psi(x_1)\phi(y)\, dy\, dx_1\,, \\ &\frac{1}{\varepsilon^{d-1}} \int_{\Omega_\varepsilon} f_\varepsilon(x)\psi(x_1)\phi(x/\varepsilon)\, dx = \frac{1}{\varepsilon^{d-1}} \int_{\Omega_\varepsilon} \varepsilon\, g(x_1)V(x/\varepsilon)\psi(x_1)\phi(x/\varepsilon)\, dx \to 0\,. \end{aligned}$$

Since ψ was an arbitrary function, we obtain from (5.10) in the limit $\varepsilon \to 0$, for almost every $x_1 \in I$,

$$\int_{Y_2} u_0(x_1, y)[-\nabla_y \cdot (a(y)\nabla_y \phi(y) - \lambda_0 b_0(y)\phi(y)]\, dy = 0\,. \tag{5.11}$$

Since ϕ was arbitrary, this is an elliptic equation in the unit cell. Using $a = a_0$ we obtain, in the weak sense,

$$-\nabla_y \cdot (a_0(y)\nabla_y u_0(x_1, y)) - \lambda_0 b_0(y) u_0(x_1, y) = 0\,, \tag{5.12}$$

where we wrote the variable $y \in (0,2)\times\Sigma$ to illustrate the dependencies. We conclude that, for almost every $x_1 \in I$, the function $u_0(x_1,\cdot)$ is a solution of the homogeneous problem in the cell. Additionally, as a two-scale limit, it is 2-periodic in the variable y_1. Since V and W form a basis of the homogeneous solution space of this equation for 2-periodic functions (related to the wave-number $k_0 = \pi$), we obtain that $u_0(x_1,\cdot)$ has the form (5.5) with pre-factors $\alpha(x_1)$ and $\beta(x_1)$.

Item 3 is obtained by calculating the next order limits of (5.10). This means that we multiply (5.10) with ε^{-1} and investigate the limits of the integrals. We use only $\phi = \bar V$ and $\phi = \bar W$ as test-functions and perform the calculation for $\phi = \bar V$.

We start with the right-hand side of (5.10) with factor ε^{-1} and with $\phi = \bar V$. In the limit $\varepsilon \to 0$, we find, since $V(y)\bar V(y) = |V(y)|^2$ is 1-periodic in y_1,

$$\begin{aligned}\frac{1}{\varepsilon^d}\int_{\Omega_\varepsilon} f_\varepsilon(x)\psi(x_1)\bar V(x/\varepsilon)\,dx &= \frac{1}{\varepsilon^{d-1}}\int_{\Omega_\varepsilon} g(x_1)V(x/\varepsilon)\psi(x_1)\bar V(x/\varepsilon)\,dx\\ &\to \int_I\int_Y g(x_1)V(y)\psi(x_1)\bar V(y)\,dy\,dx_1\,.\end{aligned}$$

Our next aim is to investigate the terms on the left-hand side of (5.10). As a preparation, we note that $\phi = \bar V$ is a solution of the limiting eigenvalue problem, which yields

$$\begin{aligned}&-\frac{1}{\varepsilon^d}\int_{\Omega_\varepsilon} u^\varepsilon(x)\psi(x_1)(\varepsilon^2\nabla\cdot(a(x/\varepsilon)\nabla\bar V(x/\varepsilon)))\,dx\\ &\qquad= \frac{1}{\varepsilon^d}\int_{\Omega_\varepsilon} u^\varepsilon(x)\psi(x_1)\lambda_0 b_0(x/\varepsilon)\bar V(x/\varepsilon)\,dx\,.\end{aligned}\tag{5.13}$$

We now consider the first integral on the left-hand side of (5.10), with a factor ε^{-1} and for $\phi = \bar V$. We insert the left-hand side of (5.13) to generate a bounded limit. We calculate, using once more that the coefficient a is x-independent,

$$\begin{aligned}&\frac{1}{\varepsilon^d}\int_{\Omega_\varepsilon} u^\varepsilon(x)(\varepsilon^2\nabla\cdot(a(x/\varepsilon)\nabla[\psi(x_1)\bar V(x/\varepsilon)]))\,dx\\ &\qquad-\frac{1}{\varepsilon^d}\int_{\Omega_\varepsilon} u^\varepsilon(x)\psi(x_1)(\varepsilon^2\nabla\cdot(a(x/\varepsilon)\nabla\bar V(x/\varepsilon)))\,dx\\ &= \frac{1}{\varepsilon^d}\int_{\Omega_\varepsilon} u^\varepsilon(x)\varepsilon\, 2\psi'(x_1)\partial_{y_1}(a\bar V)(x/\varepsilon)\,dx + O(\varepsilon)\\ &\to \frac{1}{2}\int_I\int_{Y_2} u_0(x_1,y)\,2\psi'(x_1)\partial_{y_1}(a\bar V)(y)\,dy\,dx_1\\ &= \int_I \alpha(x_1)\psi'(x_1)\int_Y V(y)2\partial_{y_1}(a\bar V)(y)\,dy\,dx_1\\ &\qquad+\int_I \beta(x_1)\psi'(x_1)\int_Y W(y)2\partial_{y_1}(a\bar V)(y)\,dy\,dx_1\,.\end{aligned}$$

We turn to the analysis of the other integral on the left-hand side of (5.10) with factor ε^{-1} and for $\phi = \bar V$. We insert the same leading order term, now in the form of the right-hand side of (5.13). In the limit $\varepsilon \to 0$, we find, because of $(\lambda_\varepsilon - \lambda_0)/\varepsilon \to \mu$ and $(b_\varepsilon - b_0)/\varepsilon \to B$,

$$\begin{aligned}&\frac{1}{\varepsilon^d}\int_{\Omega_\varepsilon} u^\varepsilon(x)\lambda_\varepsilon b_\varepsilon(x/\varepsilon)\psi(x_1)\bar V(x/\varepsilon)\,dx\\ &\qquad-\frac{1}{\varepsilon^d}\int_{\Omega_\varepsilon} u^\varepsilon(x)\psi(x_1)\lambda_0 b_0(x/\varepsilon)\bar V(x/\varepsilon)\,dx\end{aligned}$$

$$
\begin{aligned}
&\to \frac{1}{2}\int_I\int_{Y_2} u_0(x_1,y)\mu b_0(y)\psi(x_1)\bar V(y)\,dy\,dx_1\\
&\quad + \lambda_0\frac{1}{2}\int_I\int_{Y_2} B(\,\cdot\,)(u_0(x_1,\,\cdot\,)\psi(x_1)\bar V(\,\cdot\,))\,dy\,dx_1\\
&= \int_I\int_Y (\alpha(x_1)V(y)+\beta(x_1)W(y))\mu b_0(y)\psi(x_1)\bar V(y)\,dy\,dx_1\\
&\quad + \lambda_0\int_I\left\{\alpha(x_1)\int_Y BV\bar V\,dy + \beta(x_1)\int_Y BW\bar V\,dy\right\}\psi(x_1)\,dx_1\,.
\end{aligned}
$$

We can now combine the three limit expressions that are obtained from (5.10). Since ψ was arbitrary, we obtain, for a.e. $x_1 \in I$,

$$
\begin{aligned}
&\alpha'(x_1)\int_Y V(y)2\partial_{y_1}(a\bar V)(y)\,dy + \beta'(x_1)\int_Y W(y)2\partial_{y_1}(a\bar V)(y)\,dy\\
&- \alpha(x_1)\mu\int_Y b_0(y)V(y)\bar V(y)\,dy - \beta(x_1)\mu\int_Y b_0(y)W(y)\bar V(y)\,dy\\
&- \lambda_0\alpha(x_1)\int_Y BV\bar V - \lambda_0\beta(x_1)\int_Y BW\bar V = g(x_1)\int_Y V(y)\bar V(y)\,dy\,.
\end{aligned}
\tag{5.14}
$$

We did not perform simplifications such as $V\bar V = |V|^2$; the above equation remains valid when we replace everywhere the factor $\phi = \bar V$ by the factor $\phi = \bar W$.

We now continue with $\phi = \bar V$ and insert values for integrals to simplify the expression. In the first integral we use that the flux integral is $\int_Y V(y)\partial_{y_1}(a\bar V)(y)\,dy = -iF$. The second integral vanishes, the argument is given in Appendix A, see (A.1). The third integral is 1 and the fourth integral vanishes, these are consequences of the fact that V and W are b_0-orthonormal. The value of the integral on the right-hand side is abbreviated with $m = \|V\|^2_{L^2(Y)}$. We obtain an ordinary differential equations for α:

$$
-2iF\alpha'(x_1) - \alpha(x_1)\mu - \alpha(x_1)\lambda_0\int_Y BV\bar V - \beta(x_1)\lambda_0\int_Y BW\bar V = m\,g(x_1)\,. \tag{5.15}
$$

A multiplication with $i/(2F)$ yields (5.6) with the coefficients p and q of (5.8)–(5.9).

Equation (5.7) for β follows when we replace in relation (5.14), in all the seven instances, the function $\bar V$ by $\bar W$.

Item 4. We observed that F is real for constant a after (2.11). The formula for p uses the real quantities F, μ, λ_0, B, and $V\bar V = |V|^2$; this shows that p is real. When b_ε satisfies (i) of Assumption 2.2, then $B(\cdot + e_1/2) = -B(\cdot)$ together with $|V(\cdot + e_1/2)| = |V(\cdot)|$ implies $\int_Y BV\bar V = \int_Y B|V|^2 = 0$. This yields for p the simple expression $p = \mu/(2F)$.

We recall that $W = \bar V$ holds independent of symmetries. The symmetry (ii) provides directly $B(e_1 - \cdot) = B(\cdot)$, and it implies $\bar V^2(e_1 - \cdot) = V^2(\cdot)$, see the discussion after (2.10). We can therefore write the integral in the expression for q as $\int_Y B\bar V^2 = \int_{Y_{1/2}} B\bar V^2 + \int_{Y_{1/2}} B(e_1 - \cdot)\bar V^2(e_1 - \cdot) = \int_{Y_{1/2}} B\bar V^2 + \int_{Y_{1/2}} BV^2$. This shows that q is real.

The boundary conditions are derived by considering a test-function ψ that does not necessarily have compact support in I. This introduces an additional term in (5.10), namely, for the right boundary $\Gamma_\varepsilon = \{r_\varepsilon\} \times \varepsilon\Sigma$, in leading order in ε, an expression that involves the integral

$$
\int_{\Gamma_\varepsilon} u^\varepsilon(x)a(x/\varepsilon)\psi(r)\partial_{y_1}\phi(x/\varepsilon)\,dS(x)\,.
$$

In general, it is not clear how to continue the calculations with this term.

In symmetric media, as discussed after (2.10), we have $W(x_1, \tilde{x}) = V(1 - x_1, \tilde{x})$. This implies that the test-function $\phi := \bar{V} + \bar{W}$ satisfies at the position $r_\varepsilon \in \varepsilon\mathbb{Z}$ of the right boundary the identity $\partial_{y_1}\phi = \partial_{y_1}\bar{V} + \partial_{y_1}\bar{W} = \partial_{y_1}\bar{V} - \partial_{y_1}\bar{V} = 0$. The term is vanishing in r_ε and also in $-r_\varepsilon$. This implies that, when we use this test-function ϕ, no boundary terms appear.

The calculation of Item 3 implies $\int_I (2iF\alpha - 2iF\beta)\psi' = \int_I (2iF\alpha' - 2iF\beta')\psi$ for smooth functions ψ that are not vanishing at $x_1 = r_*$ or $x_1 = -r_*$. This implies $2iF\alpha - 2iF\beta = 0$ in these points and thus the boundary condition as claimed in Item 4 for bounded intervals.

The condition in the case $r_* = \infty$ is a consequence of the lower semicontinuity of the L^2-norm with respect to weak convergence. □

We add the following remark concerning boundary conditions. Since $|\alpha|$ is a measure for the energy flux to the right and $|\beta|$ is a measure for the flux to the left, for Neumann boundary conditions, we always expect the condition $|\alpha| = |\beta|$ at the boundaries, independent of symmetry assumptions. The boundary conditions that are found in Item 4 are much stronger: Not only do the absolute values coincide, but the complex numbers coincide.

6 Proof of Theorem 1.2

We prepare the proof of Theorem 1.2 by results on bounded domains.

6.1 Results on a bounded domain

The original equation (1.1) with a right-hand side f for the spectral value $\lambda = \lambda_0$, with constant coefficients a and with perturbed coefficients b_ε, reads $-\nabla\cdot(a\,\nabla u) - \lambda_0\, b_\varepsilon\, u = f$. We consider this equation for $\varepsilon > 0$ on a bounded domain $(-R, R) \times \Sigma$ for $R \in \mathbb{N}$ and with homogeneous Neumann boundary conditions along all boundaries. We introduce the corresponding solution operator $\mathcal{L} : f \to u$. We regard it here as a linear map $\mathcal{L} : X \to X$ for the function space $X := L^2((-R, R) \times \Sigma)$.

Our first result is that the sequence of solution operators is unbounded.

Lemma 6.1 (Unbounded sequence of solution operators)**.** *Let Assumption 1.1 be satisfied. We consider the combined medium, Medium I for $x_1 > 0$ and Medium II for $x_1 < 0$. We demand $\int_Y BV^2 \neq 0$ such that $q \neq 0$ is satisfied. Let $0 < \varepsilon_j \to 0$ and $\mathbb{N} \ni R_j \to R_* \in \mathbb{N} \cup \{\infty\}$ be two sequences with $\varepsilon_j R_j \geq \gamma > 0$ for all j. Let $\mathcal{L}_j : f \mapsto u$ be the solution operator as described above for the parameter $R = R_j$ and $\varepsilon = \varepsilon_j$. Then, the family*

$$\varepsilon_j\, \|\mathcal{L}_j\| \qquad \text{is unbounded.} \tag{6.1}$$

Proof. For $\varepsilon = \varepsilon_j$, we consider rescaled domains $\Omega_\varepsilon = (-r, r) \times \varepsilon\Sigma$ with geometrical parameter $r := r_j := \varepsilon_j R_j$, and the corresponding solution operators $\mathcal{L}_\varepsilon : f_\varepsilon \to u^\varepsilon$. The norm of $\mathcal{L}_\varepsilon : L^2(\Omega_\varepsilon) \to L^2(\Omega_\varepsilon)$ coincides with the norm of $\mathcal{L}_j$ on the original domain.

We choose a subsequence such that $r_j = \varepsilon_j R_j \to r_* \in \mathbb{R}_* \cup \{\infty\}$. We furthermore choose a non-vanishing non-negative function $g : \mathbb{R} \to \mathbb{R}$ with compact support in $(-r_*, r_*)$. Given g, we study the right-hand side f_ε as in (5.2) and the corresponding solution sequence $u^\varepsilon = \mathcal{L}_\varepsilon(f_\varepsilon)$. Since f_ε has typical values of order ε and the domain has a volume of order ε^{d-1}, there holds

$$\varepsilon^{-(d-1)} \| f_\varepsilon \|^2_{L^2(\Omega_\varepsilon)} = \varepsilon^{-(d-1)} \int_{\Omega_\varepsilon} |f_\varepsilon|^2 \le C\varepsilon^2 \,. \tag{6.2}$$

Property (6.1) follows when the family $\varepsilon^{-(d-1)} \| u^\varepsilon \|^2_{L^2(\Omega_\varepsilon)}$ is unbounded.

We will show this fact with a contradiction argument. We therefore assume that, for some sequence $\varepsilon \to 0$, the solution sequence u^ε satisfies

$$\varepsilon^{-(d-1)} \| u^\varepsilon \|^2_{L^2(\Omega_\varepsilon)} \le C \tag{6.3}$$

for some $C > 0$. Our aim is to derive a contradiction.

We note that (6.3) is exactly the boundedness assumption (5.3), we can therefore apply Theorem 5.1. We use the sequence $\lambda_\varepsilon = \lambda_0$ such that the rescaled limit value is $\mu = 0$. The symmetries (i) and (ii) of Assumption 2.2 are satisfied since Assumption 1.1 holds; we therefore have $p = \mu/(2F) = 0$ and $0 \neq q \in \mathbb{R}$.

Case 1: $r_* \in \mathbb{R}$. Theorem 5.1 provides that, possibly along a further subsequence, u^ε converges weakly in two scales to $u_0(x_1, y) = \alpha(x_1)V(y) + \beta(x_1)W(y)$, where (α, β) satisfies (5.6)–(5.7) on the interval $(-r_*, r_*)$, and the boundary conditions. Since g is non-vanishing and non-negative and p has the critical parameter value $p = 0$, by Proposition 4.1, there is no solution (α, β). This is the desired contradiction.

Case 2: $r_* = \infty$. Theorem 5.1 provides a limit function $u_0(x_1, y) = \alpha(x_1)V(y) + \beta(x_1)W(y)$ for $x_1 \in \mathbb{R}$, where (α, β) satisfies (5.6)–(5.7) on the interval $\mathbb{R}$ and $\alpha, \beta \in L^2(\mathbb{R})$. By the last statement of Proposition 4.1, since g is non-vanishing and non-negative and p has the critical parameter value, there is no such solution (α, β). This is the desired contradiction. □

We can now formulate a result on bounded domains that is closely related to Theorem 1.2.

Theorem 6.2 (Existence of interface modes on bounded domains)**.** *Let Assumption 1.1 be satisfied. We consider once more the combined medium and assume* $q \neq 0$*. Let* $\eta_0 > 0$ *be arbitrary. Then, there exists* $\varepsilon_0 > 0$ *such that, for every* $\varepsilon \in (0, \varepsilon_0)$ *and every* $R \in \mathbb{N}$ *with* $R \ge 1/\varepsilon$*, the Neumann problem on the domain* $(-R, R) \times \Sigma$ *in the combined medium has an eigenvalue in the interval* $(\lambda_0 - \varepsilon\eta_0, \lambda_0 + \varepsilon\eta_0)$*.*

Proof. For fixed $\eta_0 > 0$, the statement of the theorem may be written briefly as

$$\exists \varepsilon_0 > 0 \; \forall \varepsilon \in (0, \varepsilon_0)\,, R \ge 1/\varepsilon \; \exists \text{ eigenvalue } \tilde\lambda \in (\lambda_0 - \varepsilon\eta_0, \lambda_0 + \varepsilon\eta_0)\,. \tag{6.4}$$

We will argue by contradiction. We want to find a contradiction when we assume

$$\forall \varepsilon_0 > 0 \; \exists \varepsilon \in (0, \varepsilon_0)\,, R \ge 1/\varepsilon \; \forall \tilde\lambda \in (\lambda_0 - \varepsilon\eta_0, \lambda_0 + \varepsilon\eta_0) : \; \tilde\lambda \text{ is no eigenvalue}\,. \tag{6.5}$$

Assuming that (6.5) holds, we use it for $j \in \mathbb{N}$ with $\varepsilon_0 := 1/j$. This provides $\varepsilon_j < 1/j$ and $R_j \ge 1/\varepsilon_j$ such that there exists no eigenvalue in the interval $(\lambda_0 - \varepsilon_j\eta_0, \lambda_0 + \varepsilon_j\eta_0)$.

The problem on $\Omega_j = (-R_j, R_j) \times \Sigma$ has the form $(A_j - \lambda B_j)(u) = f$ where A_j is a symmetric elliptic operator. On L^2-spaces, the operator A_j has a self-adjoint compact inverse and B_j has a continuous inverse. The spectral properties of self-adjoint compact operators imply that there exists a family of orthonormal eigenfunctions Ψ_ℓ with corresponding eigenvalues Λ_ℓ for the operator A_j in the sense that $A_j \Psi_\ell = \Lambda_\ell B_j \Psi_\ell$. This implies that the solution operator $\mathcal{L}_j : f \mapsto u$ where u solves $(A_j - \lambda B_j)(u) = f$ has the form

$$\mathcal{L}_j : f \mapsto u = \sum_\ell \langle B_j^{-1} f, \Psi_\ell \rangle \frac{1}{\Lambda_\ell - \lambda} \Psi_\ell \,.$$

The solution operator $\mathcal{L}_j$ hence satisfies $\|\mathcal{L}_j\| \le \|B_j^{-1}\| / \min_\lambda |\Lambda_\ell - \lambda|$. In our setting, $\|B_j^{-1}\| \le C$ holds for some constant $C > 0$, for all $j \in \mathbb{N}$.

We recall that we assumed to be in the situation that there exists no eigenvalue in the interval $(\lambda_0 - \varepsilon_j \eta_0, \lambda_0 + \varepsilon_j \eta_0)$. This implies that the norm of the solution operator $\mathcal{L}_j$ to the problem on Ω_j is bounded by $C/(\varepsilon_j \eta_0)$. This is in contradiction with Lemma 6.1. □

6.2 Unbounded domain and proof of the main result

Proof of Theorem 1.2. We use $\eta_0 > 0$ of the spectral gap assumption in Theorem 1.2. The number ε_0 is chosen as in Theorem 6.2 for $\eta_0/2$. Our aim is to derive the statement of Theorem 1.2 with this value of ε_0. From now on, we consider an arbitrary $\varepsilon < \varepsilon_0$.

Let $R_j \to \infty$ be a sequence with $R_j \ge 1/\varepsilon$ for all j. Theorem 6.2 provides a sequence of eigenvalues $\tilde\lambda_j \in (\lambda_0 - \varepsilon\eta_0/2, \lambda_0 + \varepsilon\eta_0/2)$ with corresponding $L^2((-R_j, R_j) \times \Sigma)$-normalized eigenfunctions u_j. For a subsequence $j \to \infty$, we find a limit for the eigenvalues, $\tilde\lambda_j \to \tilde\lambda \in [\lambda_0 - \varepsilon\eta_0/2, \lambda_0 + \varepsilon\eta_0/2]$. Choosing possibly another subsequence, we find a limit function $\tilde u \in L^2(\mathbb{R} \times \Sigma)$ such that the sequence u_j converges, on every subset $(-L, L) \times \Sigma$, weakly to $\tilde u$. As a limit of solutions, also $\tilde u$ is a solution of the eigenvalue problem (for $\lambda = \tilde\lambda$).

In order conclude the statement of Theorem 1.2, it remains to verify that $\tilde u$ is an eigenfunction – we have to prove $\tilde u \neq 0$. This is not a trivial task, but it can be obtained from standard theory on periodic wave-guides, see [11, 18] and the references therein. We emphasize that we can use these theories even though the medium under consideration is not periodic. We will use Theorem 3.8 of [18], which provides an estimate for solutions u of inhomogeneous Helmholtz equations in periodic waveguides (the coefficient λb here is $k^2 n$ in [18]). We apply the theorem for λ in the spectral gap, this implies that the space Y of [18] is trivial. For a right-hand side f with support in a fixed compact set, the estimate reads $\|u\|_{H^1(\mathbb{R}\times\Sigma)} \le C\|f\|_{L^2(\mathbb{R}\times\Sigma)}$. A priori, the constant C depends on λ, but a straighforward contradiction argument provides that C can be chosen independent of λ when λ varies only in a compact interval inside a spectral gap.

Our aim now is to conclude, in our setting, that the limit function is non-trivial, $\tilde u \neq 0$. We argue by contradiction. We therefore assume that the local L^2-limit $\tilde u$ of the sequence u_j vanishes. We note that, as solutions of elliptic equations, the sequence u_j has additional regularity and converges, for arbitrary $L > 0$, strongly in $H^1((-L, L) \times \Sigma)$.

We use a cut-off function $\vartheta : \mathbb{R} \to \mathbb{R}$ of class C^2 with the properties $\vartheta(x_1) = 0$ for all $x_1 \le 0$ and $\vartheta(x_1) = 1$ for all $x_1 \ge 1$. The functions $U_j(x) := u_j(x)\vartheta(x_1)$ satisfy an inhomogeneous Helmholtz equation in a periodic medium. In order to apply periodic media results such as [18], it is important that U_j solves indeed a problem in a (single) periodic medium; but this is indeed the case since the function is vanishing for $x_1 < 0$ and it hence solves the Helmholtz-problem also for the $(x_1 > 0)$-medium.

The cut-off function ϑ introduces a right-hand side F_j on the segment $(0, 1) \times \Sigma$, the function F_j consists of products of first and second derivatives of ϑ with u_j and derivatives of u_j. By our assumption $\tilde{u} = 0$, there holds $F_j \to 0$ in $L^2((0, 1) \times \Sigma)$. Theorem 3.8 of [18] yields $\|U_j\|_{H^1(\mathbb{R}\times\Sigma)} \le C\|F_j\|_{L^2((0,1)\times\Sigma)} \to 0$. This provides that u_j converges strongly in the right part of the waveguide, $\|u_j\|_{L^2((1,\infty)\times\Sigma)} \to 0$.

The argument can be repeated with a cut-off function that vanishes for $x_1 \ge 0$. This yields $\|u_j\|_{L^2((-\infty,-1)\times\Sigma)} \to 0$. The assumption of a local trivial limit yields directly $\|u_j\|_{L^2((-1,1)\times\Sigma)} \to 0$. When we combine these three convergences, we find a contradiction to the fact that u_j is an L^2-normalized sequence. □

A Flux integrals

In this appendix we derive the relation

$$\int_Y W(y)\, \partial_{y_1}(a\bar{V})(y)\, dy = 0\,. \tag{A.1}$$

We recall the relevant properties of V and W. Both functions are $k = \pi$ quasiperiodic on the 1-cell Y in the sense that $V(\cdot + e_1) = -V(\cdot)$ and $W(\cdot + e_1) = -W(\cdot)$. Moreover, as they are constructed for the unperturbed medium, they are additionally quasiperiodic on the 1/2-cell $Y_{1/2}$ in the sense that $V(\cdot + e_1/2) = iV(\cdot)$ and $W(\cdot + e_1/2) = -iW(\cdot)$. They satisfy $W = \bar{V}$ and they are b_0-orthonormal.

These properties allow to calculate the complex conjugate of the integral in (A.1):

$$\begin{aligned}
\int_Y \bar{W}(y)\, \partial_{y_1}(aV)(y)\, dy &= \int_Y V(y)\, \partial_{y_1}(aV)(y)\, dy \\
&= \int_{\{x_1<1/2\}} V(y)\, \partial_{y_1}(aV)(y)\, dy + \int_{\{x_1<1/2\}} V(y + e_1/2)\, \partial_{y_1}(aV)(y + e_1/2)\, dy \\
&= \int_{\{x_1<1/2\}} V(y)\, \partial_{y_1}(aV)(y)\, dy - \int_{\{x_1<1/2\}} V(y)\, \partial_{y_1}(aV)(y)\, dy = 0\,.
\end{aligned}$$

This shows the claimed property (A.1).

References

[1] G. Allaire. "Homogenization and two-scale convergence". *SIAM J. Math. Anal.* 23.6 (1992), pp. 1482–1518. DOI: 10.1137/0523084.

[2] G. Bal. "Continuous bulk and interface description of topological insulators". *Journal of Mathematical Physics* 60.8 (2019).

[3] G. Bouchitté and B. Schweizer. "Homogenization of Maxwell's equations in a split ring geometry". *Multiscale Model Simul* 8.3 (2010), pp. 717–750. DOI: 10.1137/09074557X.

[4] B. Brown et al. “Spectrum created by line defects in periodic structures”. *Math. Nachr.* 287.17-18 (2014), pp. 1972–1985. DOI: 10.1002/mana.201300165.

[5] A. Drouot. “Microlocal analysis of the bulk-edge correspondence”. *Comm. Math. Phys.* 383.3 (2021), pp. 2069–2112. DOI: 10.1007/s00220-020-03864-4.

[6] A. Drouot and M. Weinstein. “Edge states and the valley Hall effect”. *Adv. Math.* 368 (2020), pp. 107142, 51. DOI: 10.1016/j.aim.2020.107142.

[7] A. Drouot. “The bulk-edge correspondence for continuous honeycomb lattices”. *Comm. Partial Differential Equations* 44.12 (2019), pp. 1406–1430. DOI: 10.1080/03605302.2019.1643362.

[8] V. Duchêne, I. Vukićević, and M. Weinstein. “Homogenized description of defect modes in periodic structures with localized defects”. *Commun. Math. Sci.* 13.3 (2015), pp. 777–823. DOI: 10.4310/CMS.2015.v13.n3.a9.

[9] A. Figotin and A. Klein. “Midgap defect modes in dielectric and acoustic media”. *SIAM J. Appl. Math.* 58.6 (1998), pp. 1748–1773. DOI: 10.1137/S0036139997320536.

[10] N. Filonov. “Gaps in the spectrum of the Maxwell operator with periodic coefficients”. *Comm. Math. Phys.* 240.1-2 (2003), pp. 161–170. DOI: 10.1007/s00220-003-0904-7.

[11] S. Fliss and P. Joly. “Solutions of the time-harmonic wave equation in periodic waveguides: asymptotic behaviour and radiation condition”. *Arch. Ration. Mech. Anal.* 219.1 (2016), pp. 349–386. DOI: 10.1007/s00205-015-0897-3.

[12] G. Graf and C. Tauber. “Bulk-edge correspondence for two-dimensional Floquet topological insulators”. *Ann. Henri Poincaré* 19.3 (2018), pp. 709–741. DOI: 10.1007/s00023-018-0657-7.

[13] M. Groves. “Examples of embedded eigenvalues for problems in acoustic waveguides”. *Math. Methods Appl. Sci.* 21.6 (1998), pp. 479–488. DOI: 10.1002/(SICI)1099-1476(199804)21:6<479::AID-MMA950>3.0.CO;2-V.

[14] F. Haldane and S. Raghu. “Possible Realization of Directional Optical Waveguides in Photonic Crystals with Broken Time-Reversal Symmetry”. *Physical Review Letters* 100.1 (Jan. 2008). DOI: 10.1103/physrevlett.100.013904.

[15] Y. Hatsugai. “Chern number and edge states in the integer quantum Hall effect”. *Phys. Rev. Lett.* 71 (22 Nov. 1993), pp. 3697–3700. DOI: 10.1103/PhysRevLett.71.3697.

[16] A. Kirsch and B. Schweizer. “Spectral gap properties of perturbed periodic media”. *IMA J. Appl. Math.* 90.6 (2025), pp. 595–627. DOI: 10.1093/imamat/hxag002.

[17] A. Kirsch and B. Schweizer. “Time harmonic Maxwell’s equations in periodic waveguides”. *Archive for Rational Mechanics and Analysis* 249.3 (2025). DOI: 10.1007/s00205-025-02099-8.

[18] A. Kirsch and B. Schweizer. “Periodic waveguides revisited: Radiation conditions, limiting absorption principles, and the space of bounded solutions”. *Mathematical Methods in the Applied Sciences* 48.2 (2025), pp. 2267–2293. DOI: 10.1002/mma.10435.

[19] J. Lee-Thorp, M. Weinstein, and Y. Zhu. “Elliptic operators with honeycomb symmetry: Dirac points, edge states and applications to photonic graphene”.

Arch. Ration. Mech. Anal. 232.1 (2019), pp. 1–63. DOI: 10.1007/s00205-018-1315-4.

[20] J. Lin and H. Zhang. "Mathematical theory for topological photonic materials in one dimension". *Journal of Physics A: Mathematical and Theoretical* 55.49 (Dec. 2022), p. 495203. DOI: 10.1088/1751-8121/aca9a5.

[21] R. Lipton and R. Viator. "Creating Band Gaps in Periodic Media". *Multiscale Modeling & Simulation* 15.4 (2017), pp. 1612–1650. DOI: 10.1137/16M1083396.

[22] J. Qiu et al. *Mathematical theory for the interface mode in a waveguide bifurcated from a Dirac point.* 2023. URL: https://arxiv.org/abs/2304.10843.

[23] S. Raghu and F. Haldane. "Analogs of quantum-Hall-effect edge states in photonic crystals". *Physical Review A* 78.3 (2008), p. 033834. DOI: 10.1103/PhysRevA.78.033834.

[24] M. Rudner et al. "Anomalous Edge States and the Bulk-Edge Correspondence for Periodically Driven Two-Dimensional Systems". *Phys. Rev. X* 3 (3 July 2013), p. 031005. DOI: 10.1103/PhysRevX.3.031005.

[25] B. Schweizer. "Inhomogeneous Helmholtz equations in wave guides—existence and uniqueness results with energy methods". *European J. Appl. Math.* 34.2 (2023), pp. 211–237. DOI: 10.1017/s0956792522000080.

[26] W. Su, J. Schrieffer, and A. Heeger. "Soliton excitations in polyacetylene". *Phys. Rev. B* 22 (4 Aug. 1980), pp. 2099–2111. DOI: 10.1103/PhysRevB.22.2099.

Preprints ab 2017 - 02

2026-01 **Ben Schweizer**
Edge-modes at interfaces between periodic media via reduced spatial dynamics near Dirac points

2025-04 **Bérangère Delourme, Ben Schweizer and David Wiedemann**
On polarization interface conditions for time-harmonic Maxwell's equations

2025-03 **Andreas Kirsch and Ben Schweizer**
Spectral gap properties of perturbed periodic media

2025-02 **Agnes Lamacz-Keymling, Tim Schubert and Ben Schweizer**
Existence result for Maxwell's equations in half-waveguides

2025-01 **Ben Schweizer and David Wiedemann**
Interface conditions for Maxwell's equations by homogenization of thin inclusions: transmission, reflection or polarization

2024-03 **Christian Kreuzer and Pietro Zanotti**
Inf - sup theory for the quasi - static Biot's equations in poroelasticity

2024-02 **Ben Schweizer**
Effective sound absorbing boundary conditions for complex geometries

2024-01 **Andreas Kirsch and Ben Schweizer**
Time harmonic Maxwell's equations in periodic waveguides

2023-02 **Mathias Schäffner and Ben Schweizer**
The time horizon for stochastic homogenization of the one-dimensional wave equation

2023-01 **Andreas Kirsch and Ben Schweizer**
Periodic wave-guides revisited: Radiation conditions, limiting absorption principles, and the space of bounded solutions

2022-01 **Mathias Schäffner, Ben Schweizer and Yohanes Tjandrawidjaja**
A radiation box domain truncation scheme for the wave equation

2021-02 **Klaas Poelstra, Thorsten Bartel and Ben Schweizer**
A data driven framework for evolutionary problems in solid mechanics

2021-01 **Mathias Schäffner, Ben Schweizer and Yohanes Tjandrawidjaja**
Domain truncation methods for the wave equation in a homogenization limit

2020-05 **Koondanibha Mitra, Ben Schweizer and Andreas Rätz**
Travelling wave solutions for gravity fingering in porous media flows

2020-04 **Sergio Andraus, Kilian Hermann and Michael Voit**
Limit theorems and soft edge of freezing random matrix models via dual orthogonal polynomials

2020-03 **Michael Voit and Jeannette H.C. Woerner**
Limit theorems for Bessel and Dunkl processes of large dimensions and free convolutions

2020-02 **Patrizia Donato, Agnes Lamacz and Ben Schweizer**
Sound absorption by perforated walls along boundaries

2020-01 **Christoph Schumacher**
Habilitationsschrift: Concentration inequalities in random Schrödinger operators

2019-06 **Matthias Röger and Ben Schweizer**
Relaxation analysis in a data driven problem with a single outlier

2019-05 **Klaas Hendrik Poelstra, Ben Schweizer and Maik Urban**
The geometric average of curl-free fields in periodic geometries

2019-04 **Agnes Lamacz and Ben Schweizer**
Representation of solutions to wave equations with profile functions

2019-03 **Ben Schweizer**
Existence results for the Helmholtz equation in periodic wave-guides with energy methods

2019-02 **Ben Schweizer and Maik Urban**
On a limiting absorption principle for sesquilinear forms with an application to the Helmholtz equation in a waveguide

2019-01 **Michael Voit and Jeannette H.C. Woerner**
Functional central limit theorems for multivariate Bessel processes in the freezing regime

2018-08 **Ben Schweizer**
Effective Helmholtz problem in a domain with a Neumann sieve perforation

2018-07 **Sergio Andraus and Michael Voit**
Limit theorems for multivariate Bessel processes in the freezing regime

2018-06 **Michael Voit**
Central limit theorems for multivariate Bessel processes in the freezing regime

2018-05 **Elena El Behi-Gornostaeva, Koondanibha Mitra and Ben Schweizer**
Traveling wave solutions for the Richards equation with hysteresis

2018-04 **Mario Ohlberger, Ben Schweizer, Maik Urban and Barbara Verfürth**
Mathematical analysis of transmission properties of electromagnetic meta-materials

2018-03 **Margit Rösler and Michael Voit**
Beta distributions and Sonine integrals for Bessel functions on symmetric cones

2018-02 **Michael Voit**
Continuous Association Schemes and Hypergroups

2018-01 **Merdan Artykov and Michael Voit**
Some central limit theorems for random walks associated with hypergeometric functions of type BC

2017-05 **Ben Schweizer and Florian Theil**
Lattice dynamics on large time scales and dispersive effective equations

2017-04 **Frank Klinker and Christoph Reineke**
A note on the regularity of matrices with uniform polynomial entries

2017-03 **Tomáš Dohnal and Ben Schweizer**
A Bloch wave numerical scheme for scattering problems in periodic wave-guides

2017-02 **Matthias Röger and Ben Schweizer**
Strain gradient visco-plasticity with dislocation densities contributing to the energy